



HAL
open science

PUCHI represses early meristem formation in developing lateral roots of *Arabidopsis thaliana*

Kevin Bellande, Duy-Chi Trinh, Anne-Alicia Gonzalez, Emeric Dubois, Anne-Sophie Petitot, Mikaël Lucas, Antony Champion, Pascal Gantet, Laurent Laplaze, Soazig Guyomarc'h

► To cite this version:

Kevin Bellande, Duy-Chi Trinh, Anne-Alicia Gonzalez, Emeric Dubois, Anne-Sophie Petitot, et al.. PUCHI represses early meristem formation in developing lateral roots of *Arabidopsis thaliana*. *Journal of Experimental Botany*, 2022, 73 (11), pp.3496-3510. 10.1093/jxb/erac079 . hal-03775291

HAL Id: hal-03775291

<https://hal.inrae.fr/hal-03775291>

Submitted on 5 Dec 2022

HAL is a multi-disciplinary open access archive for the deposit and dissemination of scientific research documents, whether they are published or not. The documents may come from teaching and research institutions in France or abroad, or from public or private research centers.

L'archive ouverte pluridisciplinaire **HAL**, est destinée au dépôt et à la diffusion de documents scientifiques de niveau recherche, publiés ou non, émanant des établissements d'enseignement et de recherche français ou étrangers, des laboratoires publics ou privés.



Distributed under a Creative Commons Attribution 4.0 International License

1 **Title of the manuscript:**

2 **PUCHI represses early meristem formation in developing lateral roots of *Arabidopsis***
3 ***thaliana***

4

5 **Authors**

6 Kevin Bellande¹, Duy-Chi Trinh^{1, #}, Anne-Alicia Gonzalez^{2, 3}, Emeric Dubois^{2, 3}, Anne-Sophie
7 Petitot¹, Mikaël Lucas¹, Antony Champion¹, Pascal Gantet¹, Laurent Laplaze^{1*}, Soazig
8 Guyomarc'h^{1*}

9 ¹ DIADE, Univ Montpellier, IRD, Montpellier, France

10 ² Univ Montpellier, CNRS, INSERM, Montpellier France

11 ³ Montpellier GenomiX, France Génomique, Montpellier, France

12 # Present address: Laboratoire RDP, Université de Lyon 1, ENS-Lyon, CNRS, INRAE, UCBL,
13 69364 Lyon, France.

14 * Corresponding authors: Soazig Guyomarc'h and Laurent Laplaze

15 **Email** to whom correspondence may be addressed: soazig.guyomarch@ird.fr

16

17 **Email** of all authors: kevin.bellande@ird.fr, duy-chi.trinh@ens-lyon.fr, anne-
18 alicia.gonzalez@mgx.cnrs.fr, emeric.dubois@mgx.cnrs.fr, anne-sophie.petitot@ird.fr,
19 mikael.lucas@ird.fr, antony.champion@ird.fr, pascal.gantet@ird.fr, laurent.laplaze@ird.fr,
20 soazig.guyomarch@ird.fr

21

22 **Running title:** PUCHI represses early lateral root meristem formation

23 **Date of submission:** 28 October 2021

24 **Response to reviewers:** 3 February 2022

25 **Word count:** 5169 words

26 **Number of tables and figures:** 5 figures

27 **Supplementary data:** 7 supplementary figures, 1 supplementary table

28

29 **Highlight**

30 Consistent with the hypothesis that mutual inhibition between gene regulatory sub-networks
31 contributes to lateral root formation, we show that *PUCHI* represses early meristematic gene
32 expression in developing root primordia.

33

34 **Abstract**

35 Lateral root organogenesis is a key process in the development of a plant's root system and its
36 adaptation to the environment. During lateral root formation, an early phase of cell proliferation first
37 produces a four cell-layered primordium and only from this stage onwards is a root meristem-like
38 structure, expressing root stem cell niche marker genes, being established in the developing
39 organ. Previous studies reported that the gene regulatory network controlling lateral root formation
40 is organised into two subnetworks whose mutual inhibition may contribute to organ patterning.
41 *PUCHI* encodes an AP2/ERF-transcription factor expressed early during lateral root primordium
42 development and required for correct lateral root formation. To dissect the molecular events
43 occurring during this early phase, we generated time-series transcriptomic datasets profiling lateral
44 root development in *puchi-1* mutants and wild types. Transcriptomic and reporter analyses
45 revealed that meristem-related genes were expressed ectopically at early stages of lateral root
46 formation in *puchi-1* mutants. We conclude that, consistent with the inhibition of genetic modules
47 contributing to lateral root development, PUCHI represses ectopic establishment of meristematic
48 cell identities at early stages of organ development. These findings shed light on gene network
49 properties that orchestrate correct timing and patterning during lateral root formation.

50

51 **Keywords**

52 Arabidopsis - Auxin - Cytokinin - Lateral root development - Meristem - Organogenesis - Patterning
53 - PLETHORA - PUCHI

54 **Abbreviations**

55 CHX: cycloheximide

56 DEGs: differentially expressed genes

57 DEX: dexamethasone

58 FRiP: fraction of reads in peaks

59 GR: glucocorticoid receptor

60 GO: Gene Ontology

61 GRN: gene regulatory network

62 hpg: hours post gravistimulation

63 LR: lateral root

64 LRP: lateral root primordium

65 MS: Murashige and Skoog medium

66 NAA: 1-naphthalene acetic acid

67 NPA: N-1-naphthylphthalamic acid

68 PI: propidium iodide

69 QC: quiescent centre

70 RAM: root apical meristem

71 VLCFA: very long chain fatty acids

72 WT: wild type

73

74 Introduction

75 Dynamic and plastic development evolved in sessile organisms such as plants to adapt to
76 changing environmental conditions (Morris *et al.*, 2017). Root branching, the production of new
77 lateral roots (LR) from existing roots, is key in elaborating root system architecture (Motte *et al.*,
78 2019). In the model plant *Arabidopsis thaliana*, LR arise from pre-branch sites originating in the
79 basal meristem close to the root apex (Xuan *et al.*, 2020). Primed pericycle cells at these pre-
80 branch sites enter new rounds of cell divisions producing a lateral root primordium (LRP). The
81 developing LRP, while growing through overlying cell layers, progressively organises into a new
82 root apical meristem (RAM) that ultimately emerges from the parent root and whose activity will
83 determine the later growth of the LR (Malamy *et al.*, 1997; Banda *et al.*, 2019). Remarkably, LRP
84 development is a two-step process featuring an early, so-called morphogenetic phase (stages I to
85 IV) during which cell proliferation generates a four-cell-layered, bulge-shaped LRP and a second,
86 so-called meristematic phase (stages V to VIII) when the LRP further develops to acquire key RAM
87 characteristics (Lucas *et al.*, 2013; Lavenus *et al.*, 2015; Voß *et al.*, 2015; Goh *et al.*, 2016).
88 However, the mechanisms controlling the establishment of a new root meristem and especially, the
89 transition from the early phase of LRP development to the meristematic phase, when key root
90 meristem genes start to be expressed in the centre of the developing LRP, remain unclear.

91 RAMs are proliferating tissues located at the tip of growing roots within which cell division and
92 differentiation are regulated sequentially. Maintenance of a stem cell niche at the centre of root
93 meristems ensures continuous production of cells and indeterminate organ growth (van den Berg
94 *et al.*, 1995, 1997; Bennett and Scheres, 2010; Trinh *et al.*, 2018). Multiple regulatory components,
95 including transcriptional regulators and hormones, mediate the regulation of cell identity and
96 division activity in RAMs (Himanen *et al.*, 2002; Goh *et al.*, 2012, 2016; Porco *et al.*, 2016; Du and
97 Scheres, 2017, 2018). In *A. thaliana*, networks of key transcription factors including AP2-domain
98 *PLETHORA* (*PLT*), GRAS-family transcription factors *SHORT-ROOT* (*SHR*) and *SCARECROW*
99 (*SCR*), as well as auxin-dependent factors, have been shown to control the patterning of the RAM
100 stem cell niche and specification of its organizing centre, known as the quiescent centre (QC)

101 (Galinha *et al.*, 2007; Hofhuis *et al.*, 2013; Goh *et al.*, 2016; Du and Scheres, 2017; Shimotohno *et*
102 *al.*, 2018). Many of these genes are also dynamically expressed during the process of LR
103 formation (Tian *et al.*, 2014; Lavenus *et al.*, 2015; Goh *et al.*, 2016; Du and Scheres, 2017).

104 Several studies have shown that cell fate acquisition in developing LRP is not dependent on cell
105 lineage but relies on tissue-scale mechanisms and positional signals (Lucas *et al.*, 2013; von
106 Wangenheim *et al.*, 2016). The progressive organisation of the organ could thus result from
107 emerging properties of a complex genetic network possibly integrating chemical and mechanical
108 cues (Banda *et al.*, 2019). Two examples of such patterning mechanisms are the definition of inner
109 and outer domains of the early LRP by the interplay of SHR and SCR expression domains, and the
110 correct patterning of cell divisions at early stages and transition of the developing LRP to the
111 meristematic phase by distinct sets of *PLT* genes (Goh *et al.*, 2016; Du and Scheres, 2017). These
112 data highlight that gene regulatory events during early LRP development are necessary to
113 transition to the second meristem organisation phase.

114 Inference of the gene regulatory network (GRN) during LR formation suggested that two distinct
115 genetic sub-circuits operate and that their mutual inhibition could be instrumental in LRP
116 developmental patterning (Lavenus *et al.*, 2015). The first one includes genes predominantly
117 expressed in the whole primordium in the early stages, but only in its base in the later phase. The
118 second one includes meristematic genes whose expression initiates during the transition from the
119 morphogenetic phase to the meristematic phase in the tip of the developing primordium, where the
120 new root meristem stem cell niche is established. Mutual inhibition between these two groups of
121 genes may explain the bifurcation between cell identities in the central zone and the flanking
122 domain of the developing LRP (Lavenus *et al.*, 2015). In addition, in complex genetic systems,
123 mutual inhibition motifs associated to positive regulatory cascades can generate sequential waves
124 in gene expression dynamics and control cell state switch over time (Alon, 2007).

125 *PUCHI* is an AP2/ERF-family transcription factor belonging to the first GRN sub-circuit and whose
126 loss of function or perturbation in expression kinetics impairs LRP development (Hirota *et al.*, 2007;
127 Kang *et al.*, 2013; Trinh *et al.*, 2019; Toyokura *et al.*, 2019; Goh *et al.*, 2019). GRN inference and

128 experimental validation previously revealed that PUCHI acted as a master regulator of very long
129 chain fatty acid (VLCFA) biosynthesis during the first phase of LRP development (Trinh *et al.*,
130 2019). However, the role played by PUCHI-dependent genetic pathways in LRP development
131 remains elusive.

132 Here, we show that the AP2/ERF-transcription factor PUCHI, which is predominantly expressed at
133 early stages of LR development, controls the correct timing and pattern of expression of
134 transcription factors as well as distribution of hormonal signals that orchestrate meristem formation
135 during late lateral root organogenesis. Root meristem-related genes are ectopically expressed in
136 inner cell layers of early-phase LRP in a *puchi-1* mutant background. Thus, these results support
137 the hypothesis that the inhibition of gene regulatory modules participates in LRP functional
138 patterning, and show that in the absence of PUCHI, the LR gene regulatory network yields
139 premature expression of meristematic genes in inner cells of young LRP.

140

141 **Materials and Methods**

142

143 **Plant Materials and Constructs, Growth Conditions**

144 *A. thaliana* plant ecotypes Columbia-0 (Col-0) were used for all experiments and as backgrounds
145 of transgenic lines in this study. *A. thaliana* seeds were surface-sterilized and sown on half
146 strength Murashige and Skoog ($\frac{1}{2}$ MS) solid medium with 0.7% (w/v) plant agar supplemented with
147 B5 vitamins. Plates were kept at 4°C for 2 days and then placed in long-day conditions (16-h
148 light/8-h dark cycle) in a vertical position. The *puchi-1* mutant line has previously been described
149 (Hirota *et al.*, 2007). The *promPLT:PLT-YFP* lines were reported in (Galinha *et al.*, 2007; Hofhuis *et*
150 *al.*, 2013). The *DR5::GFP* synthetic auxin response reporter was described in (Friml *et al.*, 2003),
151 the synthetic cytokinin response reporter *promTCSn::GFP* was described in (Zürcher *et al.*, 2013),
152 and the organising centre markers *QC25::CFP* and *promWOX5::nls::GFP* were described in (ten
153 Hove *et al.*, 2010) and (Goh *et al.*, 2016) respectively.

154

155 **RNAseq**

156 Col-0 wild type (WT) and *puchi-1* mutant seeds were surface-sterilized and sown on ½ MS solid
157 medium containing 0.7% (w/v) plant agar supplemented with B5 vitamins. Plates were kept at 4°C
158 for 2 days and then placed in continuous light conditions in a vertical position. Gravistimulation
159 were performed on 4-day-old seedlings and root bends were sampled at 12h, 18h, 24h, 30h and
160 36h after gravistimulation. Three biological replicates (for both Col-0 and *puchi-1*) were used for
161 the RNAseq experiment. For each replicate, root bends of more than 400 seedlings were dissected
162 under a binocular microscope and frozen in liquid nitrogen immediately on harvesting. For
163 reference, approximately 400 mature root segments located between the bend and the shoot were
164 harvested in 4-day-old seedlings at 12h after gravistimulation to be used as a reference of non-
165 gravitropic-stimulated root tissues devoid of developing LRP (termed “No LR” in the data set). Total
166 RNA was extracted using Qiagen RNeasy plant mini kit with an on-column DNase treatment
167 following the manufacturer’s recommendation (RNase-free DNase Set, Qiagen, Crawley, UK).
168 RNA samples were quantified using a Nanodrop ND100 spectrophotometer (Nanodrop,
169 Wilimington, USA) and RNA purity and integrity were evaluated using High-Resolution Automated
170 Electrophoresis 2100 Bioanalyzer system from Agilent Technologies
171 (<https://www.agilent.com/en/product/automated-electrophoresis>).

172 RNAseq analyses was performed by the MGX-Montpellier GenomiX platform
173 (<https://www.mgx.cnrs.fr/>). cDNA libraries were constructed using a Stranded mRNA Prep Ligation
174 kit (Illumina, San Diego, CA, USA) according to the manufacturer’s instructions. Briefly, poly-A
175 RNAs were purified using oligo-d(T) magnetic beads from 310 ng of total RNA. Poly-A RNAs were
176 fragmented and underwent reverse transcription using random hexamers. During the second
177 strand generation step, dUTP substituted dTTP to prevent the second strand being used as a
178 matrix during the final PCR amplification. Double stranded cDNAs were adenylated at their 3' ends
179 and ligated to Illumina's universal anchors. Ligated cDNAs were amplified following 12 PCR cycles.
180 During this PCR, the libraries were indexed, and the adapter's sequences were completed to be

181 compatible with the cluster generation step. PCR products were purified using AMPure XP Beads
182 (Beckman Coulter Genomics, Brea, CA, USA). Libraries were validated using a High Sensitivity
183 NGS kit on a Fragment Analyzer (Agilent Technologies, Santa Clara, CA, USA) and quantified
184 using a KAPA Library quantification kit (Roche, Basel, Switzerland).

185 For library sequencing, 36 libraries were pooled in equimolar amounts. The balance between all
186 samples of the pool was assessed by sequencing on a Miniseq (Illumina, San Diego, CA, USA)
187 using a 300 cycle Mid Output Reagent Cartridge. The pool was then sequenced on a Novaseq
188 6000 (Illumina, San Diego, CA, USA) S1 flow cell in paired end 2*100 nt mode according to the
189 manufacturer's instructions. This sequencing produced between 36 and 44 million passed filter
190 clusters per library.

191 For sequencing quality control, image analyses and base calling were performed using the
192 NovaSeq Control Software and Real-Time Analysis component (Illumina, San Diego, CA, USA).
193 Demultiplexing and trimming were performed using Illumina's conversion software (bcl2fastq 2.20).
194 The quality of the raw data was assessed using FastQC from the Babraham Institute and the
195 Illumina software SAV (Sequencing Analysis Viewer). FastqScreen was used to estimate the
196 potential level of contamination.

197 For alignment and statistical analysis, a splice junction mapper, TopHat 2.1.1 (Kim *et al.*, 2013)
198 (using Bowtie 2.3.5.1 (Langmead *et al.*, 2009)), was used to align the RNA-Seq reads to the *A.*
199 *thaliana* genome (NCBI TAIR10.1) with a set of gene model annotations (gff file downloaded from
200 NCBI on November 13, 2020). Final read alignments with more than 6 mismatches were
201 discarded. Samtools (v1.9) was used to sort the alignment files. Then, gene counting was
202 performed using Featurecounts 2.0.0 (Liao *et al.*, 2014). As the data is from a strand-specific
203 assay, the reads needed to be mapped to the opposite strand of the gene (-s 2 option). Before
204 statistical analysis, genes with less than 15 reads (cumulating all the analysed samples) were
205 filtered out.

206 Differentially expressed genes (DEGs) were identified using the Bioconductor (Gentleman *et al.*,
207 2004) package (<http://www.bioconductor.org>) DESeq2 1.26.0 (Love *et al.*, 2014) (R version 3.6.1).

208 Data were normalised using the DESeq2 normalisation method. Genes with an adjusted p-value of
209 less than 5% (according to the False Discovery Rate method by Benjamini-Hochberg) were
210 declared differentially expressed. DEGs between Col-0 and *puchi-1* were then investigated for
211 each time point. The DEGs with a Log2Fold-change ≥ 1 and a DESeq2 package-Wald Test (*p*-
212 value: $p^* < 0.05$; $p^{**} < 0.02$; $p^{***} < 0.01$) were selected for the gene ontology (GO) analysis. GO
213 biological process enrichment analyses of either, the list of up- or down-regulated DEGs in *puchi-1*
214 were performed using a PANTHER Overrepresentation assay (<http://pantherdb.org>) and Fisher's
215 test followed by a Bonferroni Correction ($p^* < 0.05$) (Thomas *et al.*, 2003; Mi *et al.*, 2013). Only the
216 individual elementary annotations of the GO biological process are shown.

217

218 **RT-qPCR analysis**

219 For RT-qPCR analyses, plant material was collected following the lateral root-induction system
220 described in (Himanen *et al.*, 2002). Briefly, square Petri dishes containing $\frac{1}{2}$ MS solid medium,
221 0.7% (w/v) plant agar supplemented with B5 vitamins and containing N-1-naphthylphthalamic acid
222 (NPA) and/or 1-naphthalene acetic acid (NAA) were used. Col-0 and *puchi-1* seeds were
223 germinated and grown for 72 h on 5 μ M NPA before transfer to 5 μ M NPA-containing (control) or
224 10 μ M NAA-containing (lateral root induction) medium. Three biological replicates of root segments
225 without the root apical meristem were harvested after 24h of treatment and immediately frozen in
226 liquid nitrogen for each condition. Total RNA was extracted using a Qiagen RNeasy plant mini kit
227 with an on-column DNase treatment following the manufacturer's recommended protocol (RNase-
228 free DNase Set, Qiagen, Crawley, UK). Quantification, purity and contaminations assessment of
229 the RNA samples were tested using a gel electrophoresis and a Nanodrop ND100
230 spectrophotometer (Nanodrop, Wilimington, USA). cDNA generated from the three biological
231 replicates were synthesised following the manufacturer's recommended protocol (Omniscript RT
232 Kit, Qiagen, Crawley, UK): 1000 ng of RNA in RNase free water were heated 10min at 70°C,
233 added to the manufacturer mix (up to 20 μ L) for 1h at 37°C. Generated cDNA diluted 1/10 were
234 added to the Brilliant III Ultra-Fast SYBR® Green QPCR Master Mix with Low ROX reaction mix

235 and used to performed qPCR analysis as recommended by the manufacturer (Qiagen, Crawley,
236 UK). All qPCR reactions were carried out and analysed using the Roche® LC480 Lightcycler
237 system and software (qPCR analysis program, Cq determination, curves calibration). Complete
238 thermocycling parameters were as follow: 95°-3'15; 95°-20", 60°-20" x 40 cycles; 95°-1', 60°-30",
239 95°-30". Normalisation was achieved with the tubulin *TUB3* gene (AT5G62700) and the *UBQ5*
240 gene (AT3G62250) (Lavenus *et al.*, 2015; Trinh *et al.*, 2019). The calibrator cDNA for relative
241 quantification of the effect of each treatment was the control WT treated with NPA. Data are
242 represented as mean ± SEM (standard error of the means). Significance between NAA treated
243 samples was determined using a Student's t test ($p^* < 0.05$; $p^{**} < 0.02$; $p^{***} < 0.01$). The primers used
244 for RT-qPCR analysis were designed to generate 75-110 bases amplicon length. Primer's
245 efficiency and specificity was confirmed by qPCR. Primer sequences were as follows:

246 AT3G20840: PLT1-F caaccctttcaaacacaagagt; PLT1-R ttggaacctctcctcctca; AT1G51190: PLT2-F
247 aggaaaggaagacaagtctacttagg; PLT2-R agaggaccccaatatttaagtg; AT5G10510: PLT3-F
248 gatctttaccttggacctttgc; PLT3-R gctgctatgcatacgctca; AT5G17430: PLT4/BBM-F
249 gagacaataatagtcactcccagat; PLT4/BBM-R tttgtcgttattgtaatgtattgc; AT5G57390: PLT5-F
250 ctccatgtacagaggcgta; PLT5-R gcagcttctcttgagtgcta; AT5G65510: PLT7-F
251 aacagctgtaggaggaaggt; PLT7-R tctatcttctgtcatatccaccta; TUB3-F tgcattggtacacagggtgagggaa;
252 TUB3-R agccgtgcatcttggtattgctg; UBQ5-F cgatggatctggaaaggttc; UBQ5-R agctccacaggttgcgtag

253

254 **Confocal Microscopy, Image Processing and Analysis**

255 Confocal microscopy images were obtained with a LEICA SP8 confocal system using a 40X HCX
256 corr Plan Apochromat CS 1.1 NA water objective. Samples were mounted in water or in 15 µM
257 propidium iodide (PI) for 1-2 h or in 15 µM PI supplemented with 0.004% Triton X-100 for 20-40 min
258 as previously described (Du and Scheres, 2017). All combinatorial fluorescence analyses were run
259 as sequential scans. The following excitation/emission settings were used to obtain specific
260 fluorescence signals: for PI, 488/600 to 620 nm; for YFP, 514/520-550 nm, for CFP, 458/475-505

261 nm and for EGFP, 488/500 to 550 nm. All post-acquisition image such as channel merging was
262 performed using Fiji (<https://imagej.net/Fiji>) (Schindelin *et al.*, 2012).

263

264 **Database mining for PUCHI target genes**

265 Genes showing differential expression (fold change ≥ 1.5 , p-value ≤ 0.05 as determined by Welch
266 two sample t-test) in auxin-treated PUCHI-GR roots upon dexamethasone treatment and in
267 presence of cycloheximide were retrieved from (Trinh *et al.*, 2019). Genes associated to genome
268 sequences bound by the transcription factor PUCHI *in vitro* (ampDAP, FRiP $\geq 5\%$) were retrieved
269 from the Arabidopsis DAP-seq database published at
270 http://neomorph.salk.edu/dev/pages/shhuang/dap_web/pages/index.php (O'Malley *et al.*, 2016). List
271 contents were compared using the "Calculate and draw custom Venn diagrams" system from VIB /
272 UGent Bioinformatics & Systems ([https://bioinformatics.psb.ugent.be/cgi-](https://bioinformatics.psb.ugent.be/cgi-bin/liste/Venn/calculate_venn)
273 [bin/liste/Venn/calculate_venn](https://bioinformatics.psb.ugent.be/cgi-bin/liste/Venn/calculate_venn)) to select genes that had been detected by at least two of the three
274 methods: RNAseq profiling of *puchi-1* roots, DAP-seq using PUCHI as a bait, or inducible
275 complementation of PUCHI-GR *puchi-1* roots. Aliases and description summaries were retrieved
276 for each gene from Thalemine (<https://bar.utoronto.ca/thalemine/begin.do>). Overrepresentation of
277 Gene Ontologies among the 150 genes that are common between two datasets was assayed
278 using the PANTHER algorithm (<http://pantherdb.org>) and Fisher's test followed by a Bonferroni
279 Correction ($p^* < 0.05$) (Thomas *et al.*, 2003; Mi *et al.*, 2013). Among the list of those 150 genes,
280 transcription factors and genes annotated as related to auxin, cytokinin, VLCFA, LR development,
281 or meristem regulation were selected for closer inspection (see suppl. Table 1 for detailed lists).

282

283

284 **Results**

285

286 **Loss of PUCHI function alters sequential expression patterns of *PLETHORA* genes in** 287 **developing lateral root primordia**

288 To assess the role played by PUCHI in the genetic regulation of LRP development and identify its
289 targets, either direct or indirect, during this organogenesis process, we performed a time-series
290 transcriptomic analysis following LR induction by gravistimulation in Col-0 wild type (WT) and
291 *puchi-1* mutant plants (Fig.1A). Root segments were sampled at 12 hours post gravistimulation
292 (hpg; stage I), 18 hpg (predominantly stage II in Col-0 and *puchi-1*), 24 hpg (stages II-IV in Col-0,
293 stages II-III in *puchi-1*), 30 hpg (stages III-V in Col-0, stages II-IV in *puchi-1*) and 36 hpg (stages III-
294 VI in Col-0, stages II-V in *puchi-1*), which correspond approximately to LR initiation, the mid and
295 late morphogenetic phases, and the early meristematic phase in a Col-0 background in our
296 experimental conditions (Fig. S1A, S1B and S1C) (Goh *et al.*, 2016; Trinh *et al.*, 2019). A root
297 segment was sampled directly upward of the root bend in both genotypes at 12 hpg to be used as
298 “No LR” reference material. RNAseq profiling of these samples was performed and differentially
299 expressed genes (DEGs) between successive time points or between the 2 genotypes at a single
300 time point were identified (Log2FC > 1 or Log2FC < -1, p* < 0.05; see Material and methods
301 section).

302 A total of 5791 genes in WT and 9571 genes in the *puchi-1* mutant background were shown to be
303 differentially expressed during the LRP developmental time course. Noticeably, comparison of WT
304 and *puchi-1* reference “No LR” root segments revealed 361 genes differentially expressed between
305 the two genotypes (Fig. 1B). By contrast, comparison of *puchi-1* to WT LRP transcriptomic
306 datasets at 12, 18, 24, 30, and 36 hpg yielded a minimum of 314 up to a maximum of 1009 DEGs,
307 with the highest divergence between the two genotypes observed at 24 hpg and 36 hpg (Fig.1B).
308 Because we were first interested in uncovering the role of PUCHI in the process of lateral root
309 organogenesis without necessarily distinguishing the primary molecular targets of this transcription
310 factor from the secondary regulatory events influencing LRP formation, we examined all the genes

311 whose expression dynamics during LRP formation was shown to be dependent on PUCHI function,
312 later termed PUCHI-dependent genes.

313 We analysed gene ontology (GO) enrichment among differentially expressed genes focusing
314 specifically on genes whose expression is up-regulated in *puchi-1* as compared to WT or on genes
315 whose expression is downregulated in *puchi-1* as compared to WT. Consistent with previous
316 studies, this analysis revealed that PUCHI-dependent genes are highly enriched in lipid
317 metabolism-related genes (p -value < 0,001), and confirmed that PUCHI positively influences the
318 expression of multiple VLCFA, cutin, and suberin biosynthetic genes during LRP formation (Fig.
319 1C-D, Supp. Fig. S2, Supp. Fig. S3) (Trinh *et al.*, 2019). In addition, transcriptomic profiling in
320 *puchi-1* and WT revealed other biological processes dependent on PUCHI. Interestingly, root
321 development related genes were overrepresented in the *puchi-1* RNAseq dataset as compared to
322 WT ($p^* < 0.05$ when comparing *puchi-1* and WT at 24h). These genes include *PLT1*, *PLT2*, and
323 *PLT4/BBM* genes, which are well known regulators of root apical meristem establishment and
324 maintenance (Fig. 1D) (Aida *et al.*, 2004). Other genes whose function can be related to root
325 meristem organisation or activity (e.g., predominantly expressed in the QC (Nawy *et al.*, 2005))
326 displayed altered expression dynamics during LRP development in the *puchi-1* background (Supp.
327 Fig. S3). Especially our RNAseq analysis shows robust overexpression of *PLT1* and *PLT4* genes
328 in *puchi-1* root segments throughout the four time points of our dataset and especially at 18h and
329 24h, which corresponds to root segments harbouring young LRP from stage II to stage III, *i.e.*,
330 before the transition to the meristematic phase (Fig. 1D, Supp. Fig. S1). Conversely other
331 regulators of the PLETHORA family, *PLT5* and *PLT7*, were downregulated in *puchi-1* root
332 segments as compared to WT (Fig. 1D). These latter results are consistent with previously
333 published LR GRN prediction analyses and confirm that both *PLT5* and *PLT7* genes are positively
334 regulated downstream of *PUCHI* in the early morphogenetic phase (Lavenus *et al.*, 2015). Under
335 expression of *PLT5* and *PLT7* were confirmed by independent RT-qPCR analyses in *puchi-1* roots
336 compared to WT 24h after LR induction by auxin (which correspond to stages II-III LRP in Col-0
337 and stages I-III LRP in *puchi-1*) (Himanen *et al.*, 2002) (Supp. Fig. S4A).

338 We took advantage of published *in vitro* and *in vivo* datasets to compare identified DEGs to
339 previously reported PUCHI-dependent gene expression or PUCHI genomic binding sites. First, a
340 list of 13 putative direct target genes of PUCHI were previously identified from the transcriptomic
341 response of PUCHI-GR seedlings' roots upon dexamethasone treatment and in presence of
342 cycloheximide, an inhibitor of protein synthesis (Trinh *et al.*, 2019). Second, a total of 2412 putative
343 PUCHI binding sites have been identified in the genome using the DAP-seq technology (O'Malley
344 *et al.*, 2016). Comparison of those lists to the list of PUCHI-dependent genes identified by RNAseq
345 profiling of branching root segments (this work) yielded 1 single gene, namely *CYTOKININ*
346 *RESPONSE FACTOR 1 (CRF1)*, that is retrieved by these 3 investigation methods, and a total of
347 150 genes identified by at least two of these three experimental strategies (Supp. Fig. S5A and
348 Supp. Table 1). Because DAP-seq profiles genomic sequences for which the PUCHI transcription
349 factor displays affinity *in vitro*, and because PUCHI-GR complementation assay was performed in
350 presence of cycloheximide, *CRF1* is most likely a direct target of PUCHI, that induces its
351 expression during LRP formation (Supp. Fig. S3, Supp. Fig. S6E). Interestingly, this gene encodes
352 a component of the cytokinin signalling pathway that modulates a wide range of developmental
353 processes (Raines *et al.*, 2016) (Supp. Fig. S5). Next, a Gene Ontology analysis revealed that
354 genes associated to responses to stresses and to chemical stimuli are overrepresented among the
355 150 genes shared by at least two of these three experimental datasets (Supp. Table 1).
356 Transcription factor genes and genes associated to auxin and cytokinin homeostasis and signalling
357 pathways, LR development, meristem regulation, and VLCFA biosynthesis are also in this list
358 (Suppl. Fig. S5B and Supp. Table 1). Remarkably, *PLT5*, whose expression dynamics in branching
359 root segments is dependent on PUCHI (this work), was associated to PUCHI-binding sites
360 identified by DAP-seq analysis. Thus, altogether these results suggest that the early expressed
361 LRP regulator *PLT5* may also be a direct target gene of PUCHI during lateral root development.

362 LRP development progression in a *puchi-1* mutant background has previously been shown to be
363 delayed (Hirota *et al.*, 2007; Trinh *et al.*, 2019). To assess the role played by this developmental
364 delay in the transcriptomic gap observed between *puchi-1* and WT LRPs, we analysed the
365 expression profiles of selected genes whose time-dependent expression dynamics during LRP

366 development have previously been documented (Lavenus *et al.*, 2015; Nagata *et al.*, 2021). In
367 most cases, observed changes in gene expression kinetics between both genotypes were not
368 consistent with, simply, shifted developmental time courses (Supp. Fig. S6 and S7). Taken
369 together, our data confirm that PUCHI activity is required for correct LRP development progression
370 and suggests this transcription factor induces the expression of *CRF1*, *PLT5* and *PLT7* genes and
371 represses the expression of several meristem-specific genes during the LRP early morphogenetic
372 phase.

373

374 **Meristematic PLT genes are induced prematurely in *puchi-1* LRP**

375 It was previously reported that the transcription factors PLT3, PLT5 and PLT7 control the induction
376 of *PLT1*, *PLT2* and *PLT4* in developing LRP (Du and Scheres, 2017). Unexpectedly, *PLT1* and
377 *PLT4* were overexpressed and *PLT5* and *PLT7* downregulated in *puchi-1* mutant roots, especially
378 in the early stages of development (Fig. 1D; Supp. Fig. S4A). To analyse the impact of *PUCHI* loss
379 of function on the expression pattern of root meristem-related *PLT* genes, transgenic reporter
380 constructs *promPLT1:PLT1-YFP*, *promPLT2:PLT2-YFP*, *promPLT3:PLT3-YFP* and
381 *promPLT4:PLT4-YFP* were introduced into the *puchi-1* mutant background, and their expression
382 pattern compared to that in the WT background (Galinha *et al.*, 2007; Hofhuis *et al.*, 2013).
383 Consistent with our time-course RNAseq results, we observed earlier *PLT1-YFP* and *PLT4-YFP*
384 expression in stages II-III (18h-24h after gravistimulation) in *puchi-1* LRP compared to WT (Fig.
385 2A-F, 2G-L). Conversely, *PLT3-YFP* expression was weaker in *puchi-1* LRPs, while the *PLT2-YFP*
386 construct did not display major changes in expression in *puchi-1* compared to WT before LRP
387 emergence (Supp. Fig. S4B-G and H-M). Hence, our results reveal that PUCHI inhibits expression
388 of *PLT1* and *PLT4*, two key root meristem transcription factors, during the early stages of LRP
389 formation.

390

391 **PUCHI represses expression of QC markers during the early LR development phase**

392 During the first phase of LR organogenesis, anticlinal, periclinal and tangential cell divisions
393 progressively generate a 4-layer LRP that grows against the overlying endodermal layer (Malamy
394 *et al.*, 1997; von Wangenheim *et al.*, 2016). A major developmental transition occurs at this stage,
395 during which the LRP first expresses QC marker genes in inner central cells and acquires a dome
396 shape as it breaks through the endodermis (Lucas *et al.*, 2013; von Wangenheim *et al.*, 2016; Goh
397 *et al.*, 2016). The early expression of meristematic *PLT* genes suggests the transition from the
398 early, morphogenetic to the second, meristematic phase occurred prematurely in the *puchi-1*
399 background. To test this hypothesis and confirm modifications in QC marker gene expressions
400 observed in the RNAseq data (Supp. Fig. S3) (Nawy *et al.*, 2005), we investigated meristem
401 establishment in *puchi-1* LRP using QC marker constructs *QC25::CFP* and *promWOX5::nls:GFP*
402 (ten Hove *et al.*, 2010; Goh *et al.*, 2016). Expression of *QC25::CFP* in Col-0 LRPs was first
403 detected in a few central cells in the second outermost layer from stages IV-V onwards (Fig. 3C, E,
404 G) (Goh *et al.*, 2016; Du and Scheres, 2017). In contrast, in a *puchi-1* loss-of-function background,
405 *QC25::CFP* expression could be detected in young LRPs as early as stage II (Fig. 3B and 3D), and
406 later in a wider domain compared to WT (Fig. 3G-H). Similarly, *promWOX5::nls:GFP* was
407 expressed prematurely in stage II in inner cell layers of *puchi-1* LRPs which correlates with *WOX5*
408 upregulation observed in *puchi-1* RNAseq data as compared to WT at 18 h after LR induction (Fig.
409 3I-J; Supp. Fig. S3). Furthermore, the *promWOX5::nls:GFP* expression domain stretches to inner
410 cell layers, but also to flanking cells at later stages in *puchi-1* LRPs (Fig. 3K-P). Altogether, our
411 observations show that QC marker gene expression occurs earlier and in a wider domain in *puchi-*
412 *1* LRPs. We conclude that PUCHI is required to delay the activation of QC marker gene expression
413 during LRP development, possibly *via* repressing *PLT1* and *PLT4* expression at early stages.

414

415 **Auxin and cytokinin signalling patterns are modified in *puchi* LRP**

416 Auxin distribution regulates *PLT* gene expression and contributes to LRP organisation (Laskowski
417 *et al.*, 2008; Peret *et al.*, 2014; Mähönen *et al.*, 2014; Du and Scheres, 2017; Scheres and Krizek,
418 2018). Interestingly, our transcriptomic analysis revealed that genes induced by auxin, such as

419 *IAA2*, or encoding auxin transporters, such as *PIN1*, *PIN3*, *PIN4* and *PIN7*, were upregulated in the
420 early stages (18 hpg-24 hpg) of LRP development in *puchi-1* (Fig. 4A and Supp. Fig. S3) (Bishopp *et al.*,
421 2011). We used the *DR5::GFP* synthetic auxin response reporter to visualise the pattern of
422 auxin signalling in *puchi-1* LRP compared to WT (Friml *et al.*, 2003). As previously described
423 (Benková *et al.*, 2003), the *DR5::GFP* reporter revealed an auxin response gradient in developing
424 WT LRPs with a maximum close to the LRP tip (Fig. 4B, 4D and 4F). In *puchi-1* mutant LRP too,
425 the *DR5::GFP* reporter signal was non-uniformly distributed and displayed predominant expression
426 in the centre of the primordium in contrast to its flanks (Fig. 4C, 4E and 4G). However, in
427 comparison to the WT situation, *DR5::GFP* expression domain was broader and extended closer to
428 the LRP base in *puchi-1*, especially in primordia from stage IV onwards. Thus, in contrast to
429 previous report based on *DR5::GUS* expression pattern (Hirota *et al.*, 2007), our data suggest that
430 *PUCHI* is required for the establishment of a WT-like auxin signal gradient during LRP
431 development. We therefore investigated the spatial distribution of *PIN1* proteins in Col-0 and *puchi-*
432 *1* LRP using a *promPIN1::PIN1-GFP* construct (Benková *et al.*, 2003). This revealed *PIN1*
433 distribution is strongly impaired in *puchi-1* LRP from stage III onwards, displaying a higher signal in
434 inner cell layers compared to WT (Fig. 4H-O).

435 Previous studies have shown that cytokinin impacts *PIN1* polarization in LRP from stage III
436 onwards by reallocating *PIN1* to periclinal membranes (Marhavý *et al.*, 2011, 2014). To test
437 whether *puchi-1* LRP defects are correlated with perturbations in cytokinin signalling patterning, the
438 *promTCSn::GFP* reporter was introduced into the *puchi-1* mutant background and its expression
439 compared to that in WT LRPs (Zürcher *et al.*, 2013). In WT, *promTCSn::GFP* expression was not
440 detected in LRPs before stage VII, and from stage VII onwards the expression of this cytokinin
441 signalling reporter was restricted to pro-vascular cells as previously described (Fig. 4P, 4R and 4T
442 (Bielach *et al.*, 2012). In contrast, *promTCSn::GFP* expression was detected in central cells in the
443 inner layers and extended to flanking regions of *puchi-1* LRP from stage II onwards (Fig. 4Q). In
444 later stages, cytokinin signalling was observed in LRP flanks (Fig. 4S and 4U). We conclude that
445 *PUCHI* loss of function compromises the establishment of auxin and cytokinin response patterns in
446 developing LRPs.

447

448 **Discussion**

449

450 Two successive phases were previously described during the process of LR organogenesis before
451 the emergence of a new LR. During the first, so-called morphogenetic phase, cell proliferation
452 generates a four-cell-layered primordium that grows against the overlying endodermis layer. Only
453 at this stage, at about mid-term of the full developmental time course of the LRP, do anatomic
454 features reminiscent of the meristem stem cell niche become apparent in the centre of the
455 primordium, where expression of QC marker genes initiates (Lavenus *et al.*, 2015; Voß *et al.*,
456 2015; Goh *et al.*, 2016). Onset of QC marker gene expression at this transition stage is dependent
457 on the previous establishment of the layered pattern that is controlled by the SHR/SCR pathway
458 (von Wangenheim *et al.*, 2016; Goh *et al.*, 2016). Next, during the following developmental steps,
459 the root meristem organisation in the centre of the growing primordium becomes more and more
460 complex while surrounding cells retain LRP boundary characteristics (Malamy *et al.*, 1997;
461 Lavenus *et al.*, 2015). After LR emergence, the QC may maintain the indeterminate growth of the
462 LR by repressing differentiation of the surrounding meristematic cells as it is described in primary
463 root meristems (van den Berg *et al.*, 1995). Many transcriptional regulators were shown to be
464 dynamically expressed during the process of LR organogenesis and may participate in the control
465 of cell proliferation and the acquisition of new cell identities. Remarkably, inference of the gene
466 regulatory network controlling LR development suggested that it is organised in two genetic
467 subnetworks whose mutual inhibition may explain LRP development patterning (Lavenus *et al.*,
468 2015; Voß *et al.*, 2015). One genetic sub-circuit gathers genes, including those encoding the
469 transcription factors ARF7 and PUCHI, that are expressed at early stages in the whole primordium
470 and only in its base in later stages. The second genetic module gathers transcriptional factors such
471 as ARF5 and PLT4 whose expression spans in the central domain of the primordium where the
472 meristem stem cell niche is being established, only in the second phase of its development (Fig. 5).

473 The transcription factor PUCHI belongs to the former genetic module and is expressed very early
474 in the developing LRP from stage I (Hirota *et al.*, 2007; Trinh *et al.*, 2019; Goh *et al.*, 2019).
475 Interestingly, the correct timing of *PUCHI* induction is essential: the sequential induction of *ARF7*,
476 *LBD16*, and only then *PUCHI*, was shown to be critical for the correct progression of LR formation
477 as premature expression of *PUCHI* disrupted LRP initiation by repressing auxin-induced root
478 branching (Goh *et al.*, 2019). However, how PUCHI function at early stages influences subsequent
479 LRP development remained unclear. Here, we show that meristematic genes, *PLT1* and *PLT4*, as
480 well as root meristem QC marker constructs, *QC25::CFP* and *promWOX5::nls:GFP*, are expressed
481 ectopically at earlier stages and in wider domains in *puchi-1* developing LRP as compared to WT.
482 Conversely *PLT5* and *PLT7*, that belong together with *PUCHI* to the group of genes expressed at
483 early stages of LRP development (Lavenus *et al.*, 2015), are under-expressed in the *puchi-1* loss-
484 of-function background. Although such perturbations are not observed for all the genes in each
485 gene subnetwork, respective changes in *PLT5*, *PLT7*, and root meristem genes expression
486 patterns in *puchi-1* mutant LRPs are consistent with the hypothesis that, at the level of the LR gene
487 regulatory network system, early expressed and root meristematic genes belong to two mutually-
488 exclusive sub-circuits (Lavenus *et al.*, 2015). PUCHI participates in the induction of *PLT5* and
489 *PLT7* expression during lateral root formation, *PLT5* likely being a direct target of the transcription
490 factor PUCHI. It also shows for the first time that PUCHI, which is predominantly expressed at
491 early stages of LRP development, is required for the correct timing of meristem establishment and
492 especially represses premature expression of key meristematic genes at early stages of lateral root
493 development, namely *PLT1*, *PLT4*, and *WOX5*. Remarkably, this is clearly different from the role of
494 *PLT3*, *PLT5* and *PLT7* transcription factors which were shown to be required for the correct
495 progression of LRP development and its transition to the meristematic phase (Du and Scheres,
496 2017). This data points to a complex influence of PUCHI on the gene regulatory network controlling
497 lateral root development, as its control over the expression of its direct target genes may translate
498 into intricate effects on the gene system dynamics.

499 This raises the question of how PUCHI regulates cell identity acquisition in developing LRPs.
500 Interestingly, cross analysis of three lists of PUCHI-dependent genes highlighted *CRF1* as a likely

501 direct target gene of PUCHI. This is also supported by *in silico* predictions of PUCHI target genes
502 based on correlated, but delayed, expression profiles (Lavenus *et al.*, 2015). *CRF1* encodes an
503 AP2/ERF transcription factor that, redundantly with other CRFs, mediates part of the cytokinin
504 signalling pathway modulating various plant development processes and responses to abiotic
505 stresses, in interaction with other hormonal signalling pathways (Rashotte *et al.*, 2006).
506 Interestingly, phenotypical analyses of multiple mutant combinations and overexpressing lines
507 revealed complex and redundant influence of CRFs on primary root growth and suggested that at
508 least some members promote lateral root formation (Raines *et al.*, 2016). CRF-dependent
509 expression of PIN-family, auxin transporter genes was shown to contribute to the regulation of
510 primary root growth and lateral root formation by cytokinins (Šimášková *et al.*, 2015). The
511 expression pattern of the cytokinin reporter construct *promTCSn::GFP* and the distribution of the
512 PIN1 reporter PIN1:GFP were shown to be altered in *puchi-1* mutant LRPs as compared to WT
513 (Fig. 4). In the RNAseq profiling of LR development, *CRF1* is the only *CRF* gene displaying such
514 expression dynamics typical of the early expressed subnetwork and positively controlled by PUCHI
515 (Supp. Fig. S3). Thus, *CRF1* may represent a key target of PUCHI impacting the cytokinin and
516 auxin-dependent pathways that regulate LRP organogenesis and patterning.

517 Interestingly, a number of other transcription factors of the AP2/ERF family were identified as
518 putative PUCHI targets supported by both the RNAseq dataset and the DAP-seq dataset (*PLT5*,
519 *ERF2*, *ERF12*, *ERF53*, *ERF113*, *DDF1*) (Supp. Fig. 5B and Supp. Table 1). Transcription factors of
520 the AP2/ERF family are involved in the regulation of a wide range of developmental processes, in
521 many cases in relation with hormone or stress signalling networks (Horstman *et al.*, 2014; Feng *et al.*
522 *et al.*, 2020). Interestingly, *ERF12* was shown to regulate flower development, possibly by
523 orchestrating the sequential induction and stabilisation of reproductive developmental programs in
524 shoot apices together with PUCHI and related transcription factors (Chandler and Werr, 2020). The
525 expression dynamics of *PLT5* during LR development previously suggested that it was indeed
526 controlled by PUCHI (Lavenus *et al.*, 2005). Redundantly with *PLT3* and *PLT7*, *PLT5* was shown to
527 control cell division patterning, correct auxin signal distribution and wild type progression of LRP
528 development including the onset of root meristem gene expression such as *PLT1*, *PLT4* and

529 *WOX5* (Du and Scheres, 2017). Both *PLT5* and *PLT7* expression is downregulated in the *puchi-1*
530 mutant background, and auxin signal distribution and PIN1 localization is also impaired (Fig. 4 and
531 Supp. Fig S3). Expression of *PLT3* and/or modification in expression of *PLT5/7*-independent genes
532 in *puchi-1* may explain the observed differences between *plt3/5/7* and *puchi-1* LRP phenotypes.

533 Several genes involved in hormone homeostasis or signalling have also been identified among the
534 *PUCHI*-dependent genes (Supp. Fig S3, S5B and Supp. Table 1). Auxin and cytokinin are key
535 phytohormones whose roles in functional patterning of meristems and organ primordia have been
536 well described, although in many cases the multiple feedback loops connecting gene regulatory
537 networks and hormonal homeostasis and signalling pathways make any sequential order of
538 molecular events difficult to establish (Chandler and Werr, 2015; Salvi *et al.*, 2020). Here, we show
539 that auxin and cytokinin signalling patterns are impaired in *puchi-1* mutant LRPs. Interestingly,
540 previous reports have shown higher auxin contents in the roots of 5-day-old *puchi-1* seedlings
541 compared to WT (Goh *et al.*, 2019). Alternatively, *PUCHI* may modulate auxin signalling processes
542 and responses downstream of auxin accumulation, as suggested by the observation that ectopic
543 expression of *PUCHI* in LR founder cells compromises the auxin signal maximum establishment
544 without affecting auxin content (Goh *et al.*, 2019). More specifically, modification of auxin signalling
545 distribution in *puchi-1* mutant LRP correlates with perturbed distribution of PIN1 auxin transporters
546 (Fig. 4A and 4H-O). Formation of an auxin response gradient is critical for proper LRP
547 development (Benková *et al.*, 2003). *PLT1/2/3/4* are well-identified auxin-responsive genes that
548 regulate the establishment and maintenance of a root stem cell niche and this, in turn, regulates
549 the expression and localization of PIN transporters and therefore auxin distribution in the root
550 apical meristem and LRP (Benková *et al.*, 2003; Galinha *et al.*, 2007; Prasad *et al.*, 2011; Pinon *et*
551 *al.*, 2013; Mähönen *et al.*, 2014; Du and Scheres, 2017).

552 Cytokinins repress the expression of the PIN auxin efflux carriers in the root meristem and in LRP
553 (Laplaze *et al.*, 2007; Dello Iorio *et al.*, 2008; Růžička *et al.*, 2009; Bishopp *et al.*, 2011). In addition,
554 in the early stages of LRP development, cytokinins modulate PIN1 targeting to periclinal versus
555 anticlinal domains of cell membranes (Marhavý *et al.*, 2011, 2014). Cytokinin signal distribution,

556 PIN1 expression levels and PIN1-GFP distribution are all modified in *puchi-1* LRPs. As observed
557 for root apical meristem initiation and maintenance, or when an apical root meristem is regenerated
558 after root tip excision, auxin and cytokinin signals define complementary spatial domains that may
559 contribute to the positioning of the new stem cell niche and guide further LRP patterning (Schaller
560 *et al.*, 2015; Efroni *et al.*, 2016). This pattern is not observed in the *puchi-1* background. Altogether,
561 this suggests that compromised auxin and cytokinin response distribution in *puchi-1* LRP may
562 trigger the early ectopic expression of meristematic genes through a PIN1-regulated, auxin-
563 dependent mechanism. Alternatively, misexpression of meristematic genes in *puchi-1* LRP may
564 contribute to disorganize auxin and cytokinin signal distribution and perturb LRP morphogenesis
565 and patterning.

566 We recently showed that VLCFA biosynthetic enzymes are downstream targets of PUCHI in
567 developing LRP (Trinh *et al.*, 2019). Interestingly, an increasing body of evidence highlights cross-
568 talk between VLCFA and hormones in plant development (Boutté and Jaillais, 2020). For instance,
569 VLCFAs are involved in controlling cell proliferation in shoot organs in a cytokinin-dependent, non-
570 cell autonomous manner (Nobusawa *et al.*, 2013; Boutté and Jaillais, 2020). Furthermore, in the
571 VLCFA mutant *pasticcino1* (*pas1*), the abnormal polar distribution of PIN1 in specific cells results in
572 local alteration of auxin distribution and disturbs LRP formation (Roudier *et al.*, 2010). Last, fused
573 proliferating bulges generated by roots of *puchi* or VLCFA-defective mutants on auxin- and
574 cytokinin-supplemented medium (callus inducing medium), closely resemble that produced by
575 roots of mutants affected in polar auxin transport in response to exogenous auxin supply, as well
576 as those produced by cytokinin-overproducing pericycle upon treatment with a highly diffusible
577 auxin analog (Benková *et al.*, 2003; Geldner *et al.*, 2004; Laplaze *et al.*, 2007; Shang *et al.*, 2016;
578 Trinh *et al.*, 2019). Altogether this data suggests tight links between VLCFA, cytokinin and auxin
579 distribution and LRP patterning. Strikingly, two distinct AP2/ERF-controlled cascades targeting
580 VLCFA biosynthetic enzymes during LRP development were recently described, suggesting that
581 AP2/ERF transcription factors may act as master regulators of VLCFA biosynthesis during LRP
582 formation (Trinh *et al.*, 2019; Guyomarc'h *et al.*, 2021; Lv *et al.*, 2021). Last, VLCFA-containing
583 ceramides were recently shown to participate in a feedforward loop maintaining preferential

584 expression of the transcription factor genes *ATML1* and *PDF2*, key regulators of
585 protodermis/epidermis differentiation, in the outer cell layer of developing LRPs (Nagata *et al.*,
586 2021). This function may involve direct binding of these VLCFA-containing ceramides to the
587 START domain of the transcription factors (Nagata *et al.*, 2021). *ATML1* and *PDF2* expression
588 dynamics is lost in *puchi-1* mutant LRP (Supp. Fig S7G-H). Thus, we hypothesise that PUCHI-
589 dependent VLCFA regulation could participate actively in patterning mechanisms controlling LRP
590 organisation.

591 In conclusion, by analysing the impact of *PUCHI* loss of function on the progression of LRP
592 development and functional patterning, we showed that PUCHI is required for the correct timing of
593 meristem establishment and especially, represses premature expression of key root meristem
594 genes at early stages of LRP development. These results are consistent with the model of a LR
595 gene regulatory network organized in distinct genetic sub-circuits whose sequential inhibitions or
596 activations contribute to the transition from an early morphogenetic phase to a second, meristem-
597 establishment phase, as well as to the bifurcation between the central meristematic domain and
598 the flanking domain in the developing organ. How VLCFA-, auxin- or cytokinin-dependent
599 patterning mechanisms may interact during this process downstream of PUCHI will require further
600 investigations.

601

602 **Supplementary data**

603

604 A supplementary figure S1 shows the LRP phenotype in Col-0 and *puchi-1* LRP during the time-
605 course transcriptomic analysis after gravistimulation.

606 A supplementary figure S2 shows the list of all DEGs GO-terms enrichment during the time-course
607 transcriptomic analysis in *puchi-1* compared to Col-0 upon gravistimulation

608 A supplementary figure S3 provides the heat map of selected gene patterns up- and down-
609 regulated in *puchi-1* compared to Col-0 background during the formation of LRP.

610 A supplementary figure S4 investigates PLTs gene expression analysis in *puchi-1* compared to
611 Col-0 using q-RT PCR and confocal microscopy.

612 A supplementary figure S5 identified the PUCHI direct target genes using available datasets.

613 A supplementary figure S6 shows predicted PUCHI target gene expression patterns in *puchi-1* and
614 Col-0 background during the formation of LRP.

615 A supplementary figure S7 shows selected gene expression patterns in *puchi-1* and Col-0
616 background during the formation of LRP.

617

618 **Acknowledgments**

619

620 We thank Prof. M.J. Bennett for critical reading of the manuscript. We also thank the “Montpellier
621 Ressources Imagerie” imaging facility and Carine Alcon for providing valuable advice for confocal
622 imaging. We thank Julien Lavenus for seminal discussions about this project. This work was
623 supported by the Institute of Research for Development, the University of Montpellier, and the
624 French Agence Nationale de la Recherche through the NewRoot grant (ANR-17-CE13-0004-01).
625 MGX acknowledges financial support from the France Génomique National infrastructure, funded
626 as part of “Investissement d’Avenir” programme at the Agence Nationale de la Recherche (contract
627 ANR-10-INBS-09).

628

629 **Author contributions**

630

631 Conceptualisation: L.L., S.G.; Investigation, validation, methodology and formal analysis: K.B., T.-
632 D. C., A.-A. G., E. D., A.-S. P.; Visualization: K.B and S.G.; Writing - original draft: K.B.; Writing -
633 review & editing: K.B., T.D.C., A.-A. G., E. D., M.L., A.C., P.G., L.L., S.G.; Supervision: L.L., S.G.;
634 Funding acquisition: M.L., A.C., P.G., L.L., S.G.

635

636 **Conflict of interest**

637 The authors declare no conflict of interest.

638

639 **Funding**

640 This work was supported by the Institute of Research for Development, the University of
641 Montpellier, and the French Agence Nationale de la Recherche through the NewRoot grant (ANR-
642 17-CE13-0004-01). MGX acknowledges financial support from the France Génomique National
643 infrastructure, funded as part of “Investissement d’Avenir” programme at the Agence Nationale de
644 la Recherche (contract ANR-10-INBS-09).

645

646 **Data availability**

647

648 All data to support the conclusions of this manuscript are included in the main text and the
649 supplementary materials. The full RNA-seq data discussed in this publication have been deposited
650 in the NCBI's Gene Expression Omnibus and are accessible through GEO Series accession
651 number GSEXXXXXX.

652

References

- Aida M, Beis D, Heidstra R, Willemsen V, Blilou I, Galinha C, Nussaume L, Noh Y-S, Amasino R, Scheres B.** 2004. The PLETHORA Genes Mediate Patterning of the Arabidopsis Root Stem Cell Niche. *Cell* **119**, 109–120.
- Alon U.** 2007. Network motifs: theory and experimental approaches. *Nature Reviews Genetics* 2007 8:6 **8**, 450–461.
- Banda J, Bellande K, von Wangenheim D, Goh T, Guyomarc'h S, Laplaze L, Bennett MJ.** 2019. Lateral Root Formation in Arabidopsis: A Well-Ordered LRExit. *Trends in Plant Science* **24**, 826–839.
- Benková E, Michniewicz M, Sauer M, Teichmann T, Seifertová D, Jürgens G, Friml J.** 2003. Local, efflux-dependent auxin gradients as a common module for plant organ formation. *Cell* **115**, 591–602.
- Bennett T, Scheres B.** 2010. Root Development—Two Meristems for the Price of One? *Current Topics in Developmental Biology* **91**, 67–102.
- van den Berg C, Willemsen V, Hage W, Weisbeek P, Scheres B.** 1995. Cell fate in the Arabidopsis root meristem determined by directional signalling. *Nature* 1995 378:6552 **378**, 62–65.
- van den Berg C, Willemsen V, Hendriks G, Weisbeek P, Scheres B.** 1997. Short-range control of cell differentiation in the Arabidopsis root meristem. *Nature* 1997 390:6657 **390**, 287–289.
- Bielach A, Podlešáková K, Marhavý P, Duclercq J, Cuesta C, Müller B, Grunewald W, Tarkowski P, Benková E.** 2012. Spatiotemporal Regulation of Lateral Root Organogenesis in *Arabidopsis* by Cytokinin. *The Plant Cell* **24**, 3967–3981.
- Bishopp A, Help H, El-Showk S, Weijers D, Scheres B, Friml J, Benková E, Mähönen AP, Helariutta Y.** 2011. A mutually inhibitory interaction between auxin and cytokinin specifies vascular pattern in roots. *Current Biology* **21**, 917–926.
- Boutté Y, Jaillais Y.** 2020. Metabolic Cellular Communications: Feedback Mechanisms between Membrane Lipid Homeostasis and Plant Development. *Developmental Cell* **54**, 171–182.
- Chandler JW, Werr W.** 2015. Cytokinin–auxin crosstalk in cell type specification. *Trends in Plant Science* **20**, 291–300.
- Chandler JW, Werr W.** 2020. A phylogenetically conserved APETALA2/ETHYLENE RESPONSE FACTOR, ERF12, regulates Arabidopsis floral development. *Plant Molecular Biology* **102**, 39–54.
- Du Y, Scheres B.** 2017. PLETHORA transcription factors orchestrate de novo organ patterning during Arabidopsis lateral root outgrowth. *Proceedings of the National Academy of Sciences of the United States of America* **114**, 11709–11714.
- Du Y, Scheres B.** 2018. Lateral root formation and the multiple roles of auxin. *Journal of Experimental Botany* **69**, 155–167.
- Efroni I, Mello A, Nawy T, Ip PL, Rahni R, Delrose N, Powers A, Satija R, Birnbaum KD.** 2016. Root Regeneration Triggers an Embryo-like Sequence Guided by Hormonal Interactions. *Cell* **165**, 1721–1733.
- Feng K, Hou X-L, Xing G-M, Liu J-X, Duan A-Q, Xu Z-S, Li M-Y, Zhuang J, Xiong A-S.** 2020. Advances in AP2/ERF super-family transcription factors in plant. *Critical Reviews in Biotechnology* **40**, 750–776.
- Friml J, Vieten A, Sauer M, Weijers D, Schwarz H, Hamann T, Offringa R, Jürgens G.** 2003. Efflux-dependent auxin gradients establish the apical-basal axis of Arabidopsis. *Nature* **426**, 147–153.
- Galinha C, Hofhuis H, Luijten M, Willemsen V, Blilou I, Heidstra R, Scheres B.** 2007. PLETHORA

proteins as dose-dependent master regulators of Arabidopsis root development. *Nature* **449**, 1053–1057.

Geldner N, Richter S, Vieten A, Marquardt S, Torres-Ruiz RA, Mayer U, Jung G. 2004. Partial loss-of-function alleles reveal a role for GNOM in auxin transport-related, post-embryonic development of Arabidopsis. *Development* **131**, 389–400.

Gentleman RC, Carey VJ, Bates DM, et al. 2004. Bioconductor: open software development for computational biology and bioinformatics. *Genome Biology* **5**, R80.

Goh T, Joi S, Mimura T, Fukaki H. 2012. The establishment of asymmetry in Arabidopsis lateral root founder cells is regulated by LBD16/ASL18 and related LBD/ASL proteins. *Development (Cambridge, England)* **139**, 883–93.

Goh T, Toyokura K, Wells DM, et al. 2016. Quiescent center initiation in the Arabidopsis lateral root primordia is dependent on the SCARECROW transcription factor. *Development (Cambridge, England)* **143**, 3363–71.

Goh T, Toyokura K, Yamaguchi N, et al. 2019. Lateral root initiation requires the sequential induction of transcription factors LBD16 and PUCHI in *Arabidopsis thaliana*. *New Phytologist* **224**, 749–760.

Guyomarc'h S, Boutté Y, Laplaze L. 2021. AP2/ERF transcription factors orchestrate very long chain fatty acid biosynthesis during Arabidopsis lateral root development. *Molecular Plant* **14**, 205–207.

Himanen K, Boucheron E, Vanneste S, De Almeida Engler J, Inzé D, Beeckman T. 2002. Auxin-mediated cell cycle activation during early lateral root initiation. *Plant Cell* **14**, 2339–2351.

Hirota A, Kato T, Fukaki H, Aida M, Tasaka M. 2007. The auxin-regulated AP2/EREBP gene PUCHI is required for morphogenesis in the early lateral root primordium of Arabidopsis. *The Plant cell* **19**, 2156–68.

Hofhuis H, Laskowski M, Du Y, Prasad K, Grigg S, Pinon V, Scheres B. 2013. Phyllotaxis and rhizotaxis in Arabidopsis are modified by three plethora transcription factors. *Current Biology* **23**, 956–962.

Horstman A, Willemsen V, Boutilier K, Heidstra R. 2014. AINTEGUMENTA-LIKE proteins: hubs in a plethora of networks. *Trends in Plant Science* **19**, 146–157.

ten Hove CA, Willemsen V, de Vries WJ, van Dijken A, Scheres B, Heidstra R. 2010. SCHIZORIZA Encodes a Nuclear Factor Regulating Asymmetry of Stem Cell Divisions in the Arabidopsis Root. *Current Biology* **20**, 452–457.

Dello Ioio R, Nakamura K, Moubayidin L, Perilli S, Taniguchi M, Morita MT, Aoyama T, Costantino P, Sabatini S. 2008. A genetic framework for the control of cell division and differentiation in the root meristem. *Science* **322**, 1380–1384.

Kang NY, Lee HW, Kim J. 2013. The AP2/EREBP Gene PUCHI Co-Acts with LBD16/ASL18 and LBD18/ASL20 Downstream of ARF7 and ARF19 to Regulate Lateral Root Development in Arabidopsis. *Plant and Cell Physiology* **54**, 1326–1334.

Kim D, Pertea G, Trapnell C, Pimentel H, Kelley R, Salzberg SL. 2013. TopHat2: accurate alignment of transcriptomes in the presence of insertions, deletions and gene fusions. *Genome Biology* **14**, R36.

Langmead B, Trapnell C, Pop M, Salzberg SL. 2009. Ultrafast and memory-efficient alignment of short DNA sequences to the human genome. *Genome Biology* **10**, R25.

Laplaze L, Benkova E, Casimiro I, et al. 2007. Cytokinins act directly on lateral root founder cells to inhibit root initiation. *The Plant cell* **19**, 3889–900.

Laskowski M, Grieneisen VA, Hofhuis H, Hove CA ten, Hogeweg P, Marée AFM, Scheres B. 2008. Root System Architecture from Coupling Cell Shape to Auxin Transport (D Weigel, Ed.). *PLoS Biology* **6**, e307.

- Lavenus J, Goh T, Guyomarc'h S, et al.** 2015. Inference of the Arabidopsis lateral root gene regulatory network suggests a bifurcation mechanism that defines primordia flanking and central zones. *The Plant cell* **27**, 1368–88.
- Liao Y, Smyth GK, Shi W.** 2014. featureCounts: an efficient general purpose program for assigning sequence reads to genomic features. *Bioinformatics* **30**, 923–930.
- Love MI, Huber W, Anders S.** 2014. Moderated estimation of fold change and dispersion for RNA-seq data with DESeq2. *Genome Biology* **15**, 550.
- Lucas M, Kenobi K, Wangenheim D von, et al.** 2013. Lateral root morphogenesis is dependent on the mechanical properties of the overlaying tissues. *Proceedings of the National Academy of Sciences* **110**, 5229–5234.
- Lv B, Wei K, Hu K, et al.** 2021. MPK14-mediated auxin signaling controls lateral root development via ERF13-regulated very-long-chain fatty acid biosynthesis. *Molecular Plant* **14**, 285–297.
- Mähönen AP, Tusscher K ten, Siligato R, Smetana O, Díaz-Triviño S, Salojärvi J, Wachsmann G, Prasad K, Heidstra R, Scheres B.** 2014. PLETHORA gradient formation mechanism separates auxin responses. *Nature* **515**, 125–129.
- Malamy JE, Benfey PN, Lanctot A, Feldman TP, Moss BL, Klavins E, Villalobos LIAC, Nemhauser JL.** 1997. Organization and cell differentiation in lateral roots of Arabidopsis thaliana. *Development (Cambridge, England)* **124**, 33–44.
- Marhavý P, Bielach A, Abas L, et al.** 2011. Cytokinin Modulates Endocytic Trafficking of PIN1 Auxin Efflux Carrier to Control Plant Organogenesis. *Developmental Cell* **21**, 796–804.
- Marhavý P, Duclercq J, Weller B, Feraru E, Bielach A, Offringa R, Friml J, Schwechheimer C, Murphy A, Benková E.** 2014. Cytokinin controls polarity of PIN1-dependent Auxin transport during lateral root organogenesis. *Current Biology* **24**, 1031–1037.
- Mi H, Muruganujan A, Thomas PD.** 2013. PANTHER in 2013: Modeling the evolution of gene function, and other gene attributes, in the context of phylogenetic trees. *Nucleic Acids Research* **41**, D377–D386.
- Morris EC, Griffiths M, Golebiowska A, et al.** 2017. Shaping 3D Root System Architecture. *Current Biology* **27**, R919–R930.
- Motte H, Vanneste S, Beeckman T.** 2019. Molecular and Environmental Regulation of Root Development. *Annual Review of Plant Biology* **70**, 465–488.
- Nagata K, Ishikawa T, Kawai-Yamada M, Takahashi T, Abe M.** 2021. Ceramides mediate positional signals in Arabidopsis thaliana protoderm differentiation. *Development (Cambridge, England)* **148**.
- Nawy T, Lee J-Y, Colinas J, Wang JY, Thongrod SC, Malamy JE, Birnbaum K, Benfey PN.** 2005. Transcriptional Profile of the Arabidopsis Root Quiescent Center. *The Plant Cell* **17**, 1908–1925.
- Nobusawa T, Okushima Y, Nagata N, Kojima M, Sakakibara H, Umeda M.** 2013. Synthesis of Very-Long-Chain Fatty Acids in the Epidermis Controls Plant Organ Growth by Restricting Cell Proliferation (J Chory, Ed.). *PLoS Biology* **11**, e1001531.
- O'Malley RC, Huang S-SC, Song L, Lewsey MG, Bartlett A, Nery JR, Galli M, Gallavotti A, Ecker JR.** 2016. Cistrome and Epicistrome Features Shape the Regulatory DNA Landscape. *Cell* **165**, 1280–1292.
- Peret B, Middleton AM, French AP, et al.** 2014. Sequential induction of auxin efflux and influx carriers regulates lateral root emergence. *Molecular Systems Biology* **9**, 699–699.
- Pinon V, Prasad K, Grigg SP, Sanchez-Perez GF, Scheres B.** 2013. Local auxin biosynthesis regulation by PLETHORA transcription factors controls phyllotaxis in Arabidopsis. *Proceedings of the National*

Academy of Sciences of the United States of America **110**, 1107–12.

Porco S, Larrieu A, Du Y, et al. 2016. Lateral root emergence in Arabidopsis is dependent on transcription factor LBD29 regulation of auxin influx carrier LAX3. *Development (Cambridge, England)* **143**, 3340–9.

Prasad K, Grigg SP, Barkoulas M, et al. 2011. Arabidopsis PLETHORA Transcription Factors Control Phyllotaxis. *Current Biology* **21**, 1123–1128.

Raines T, Shanks C, Cheng C-Y, et al. 2016. The cytokinin response factors modulate root and shoot growth and promote leaf senescence in Arabidopsis. *The Plant Journal: For Cell and Molecular Biology* **85**, 134–147.

Rashotte AM, Mason MG, Hutchison CE, Ferreira FJ, Schaller GE, Kieber JJ. 2006. A subset of Arabidopsis AP2 transcription factors mediates cytokinin responses in concert with a two-component pathway. *Proceedings of the National Academy of Sciences of the United States of America* **103**, 11081–11085.

Roudier F, Gissot L, Beaudoin F, et al. 2010. Very-long-chain fatty acids are involved in polar auxin transport and developmental patterning in Arabidopsis. *Plant Cell* **22**, 364–375.

Růžička K, Šimášková M, Duclercq J, Petrášek J, Zažímalová E, Simon S, Friml J, Montagu MCEV, Benková E. 2009. Cytokinin regulates root meristem activity via modulation of the polar auxin transport. *Proceedings of the National Academy of Sciences* **106**, 4284–4289.

Salvi E, Rutten JP, Mambro RD, Polverari L, Licursi V, Negri R, Ioio RD, Sabatini S, Tusscher KT. 2020. A Self-Organized PLT/Auxin/ARR-B Network Controls the Dynamics of Root Zonation Development in Arabidopsis thaliana. *Developmental Cell* **53**, 431–443.e23.

Schaller GE, Bishopp A, Kieber JJ. 2015. The yin-yang of hormones: Cytokinin and auxin interactions in plant development. *Plant Cell* **27**, 44–63.

Scheres B, Krizek BA. 2018. Coordination of growth in root and shoot apices by AIL/PLT transcription factors. *Current Opinion in Plant Biology* **41**, 95–101.

Schindelin J, Arganda-Carreras I, Frise E, et al. 2012. Fiji: An open-source platform for biological-image analysis. *Nature Methods* **9**, 676–682.

Shang B, Xu C, Zhang X, Cao H, Xin W, Hu Y. 2016. Very-long-chain fatty acids restrict regeneration capacity by confining pericycle competence for callus formation in arabidopsis. *Proceedings of the National Academy of Sciences of the United States of America* **113**, 5101–5106.

Shimotohno A, Heidstra R, Blilou I, Scheres B. 2018. Root stem cell niche organizer specification by molecular convergence of PLETHORA and SCARECROW transcription factor modules. *Genes & development* **32**, 1085–1100.

Šimášková M, O'Brien JA, Khan M, et al. 2015. Cytokinin response factors regulate PIN-FORMED auxin transporters. *Nature Communications* **6**, 8717.

Thomas PD, Campbell MJ, Kejariwal A, Mi H, Karlak B, Daverman R, Diemer K, Muruganujan A, Narechania A. 2003. PANTHER: A library of protein families and subfamilies indexed by function. *Genome Research* **13**, 2129–2141.

Tian H, Jia Y, Niu T, Yu Q, Ding Z. 2014. The key players of the primary root growth and development also function in lateral roots in Arabidopsis. *Plant Cell Reports* **33**, 745–753.

Toyokura K, Goh T, Shinohara H, et al. 2019. Lateral Inhibition by a Peptide Hormone-Receptor Cascade during Arabidopsis Lateral Root Founder Cell Formation. *Developmental cell* **48**, 64–75.e5.

Trinh CD, Laplaze L, Guyomarc'h S. 2018. Lateral Root Formation: Building a Meristem de novo.

Annual Plant Reviews online.

Trinh DC, Lavenus J, Goh T, *et al.* 2019. PUCHI regulates very long chain fatty acid biosynthesis during lateral root and callus formation. *Proceedings of the National Academy of Sciences of the United States of America* **116**, 14325–14330.

Voß U, Wilson MH, Kenobi K, *et al.* 2015. The circadian clock rephases during lateral root organ initiation in *Arabidopsis thaliana*. *Nature Communications* **6**.

von Wangenheim D, Fangerau J, Schmitz A, Smith RS, Leitte H, Stelzer EHK, Maizel A. 2016. Rules and Self-Organizing Properties of Post-embryonic Plant Organ Cell Division Patterns. *Current Biology* **26**, 439–449.

Xuan W, De Gernier H, Beeckman T. 2020. The dynamic nature and regulation of the root clock. *Development (Cambridge)* **147**.

Zürcher E, Tavor-Deslex D, Lituiev D, Enkerli K, Tarr PT, Müller B. 2013. A robust and sensitive synthetic sensor to monitor the transcriptional output of the cytokinin signaling network in planta. *Plant Physiology* **161**, 1066–1075.

653 **Figure legends**

654 **Figure 1. Time-course transcriptomic analysis of LRP formation in Col-0 and *puchi-1* after**
655 **root gravistimulation.** (A) Schematic diagram of the experimental procedure for the RNAseq
656 analysis. (B) Number of differentially expressed genes (DEGs) in *puchi-1* compared to Col-0 at No
657 LR, 12h, 18h, 24h, 30h and 36h after gravistimulation. Genes with a fold-change of up to Log2: +/-
658 1; $p^* < 0.05$ selected. (C) Distribution of elementary Gene Ontologies (GO) among either,
659 upregulated genes or downregulated genes in *puchi* was analysed using a PANTHER
660 overrepresentation assay and Fisher test followed by a Bonferroni Correction ($p^* < 0.05$). The Heat
661 map shows the GO terms fold enrichment (FE) of DEGs for each time point. (D) Heat map of
662 selected gene patterns up- and down-regulated in *puchi-1* compared to Col-0 background during
663 the formation of LRP. Log 2-fold change (FC) of expression in *puchi-1* compared to WT is given.
664 Statistical analysis on three independent RNAseq replicates were performed using the DESeq2
665 package and Wald Test: p-value: $p^* < 0.05$; $p^{**} < 0.02$; $p^{***} < 0.01$. Colour code for the heatmaps in
666 (C) and (D) are red for upregulated genes and blue for downregulated genes. Colour code for gene
667 names in (D) indicates the module classification (Orange: module1, Morphogenetic phase and
668 Purple: module 2, Meristematic phase) as described in Lavenus *et al.*, 2015.

669

670 **Figure 2. *PUCHI* loss of function results in distinct expression patterns of meristematic**
671 **phase regulator *PLT* genes during LRP development.** (A-F) and (G-L) Expression pattern of
672 *promPLT1:PLT1-YFP* and *promPLT4:PLT4-YFP* (green) respectively in *puchi-1* and Col-0 LR
673 primordia. Stars indicate earlier detected signal expression during LRP outgrowth. Percentages
674 and numbers indicate the occurrence of the represented pattern over the total number of
675 observations. Cell walls were stained using propidium iodide (magenta). Scale bar: 25 μ m.

676

677 **Figure 3. *PUCHI* loss of function impacts QC marker gene expression patterns during LRP**
678 **formation.** Confocal microscopy images of expression of QC reporters (A-H) *QC25::CFP* and (I-P)
679 *promWOX5::nls:GFP* (green) in LRP in Col-0 and *puchi-1*. Stars indicate earlier detected signal
680 expression during LRP outgrowth. Percentages and numbers indicate the occurrence of the

681 represented pattern over the total number of observations. Cell walls were stained using propidium
682 iodide (magenta). Scale bar: 25 μ m.

683

684 **Figure 4. *PUCHI* loss of function alters auxin and cytokinin signal distribution in developing**

685 **LRP.** (A) Heat map of selected auxin transporter gene patterns upregulated in *puchi-1* compared to

686 Col-0 background during LRP formation. Log 2-fold change (FC) of expression in *puchi-1*

687 compared to WT is given. Statistical analysis on the three independent RNAseq replicates were

688 performed using the DESeq2 package and Wald Test: *p*-value: *p**<0.05; *p***<0.02; *p****<0.01. (B-G)

689 *DR5::GFP* (green), (H-O) *promPIN1::PIN1::GFP* (green) and (P-U) *promTCSn::GFP* (green)

690 expression during LR development. Percentages and numbers indicate the occurrence of the

691 represented pattern over the total number of observations. (B-M) Cell walls were stained using

692 propidium iodide (magenta). (N-U) (Inset) Signal intensity monitor. (blue) low intensity; (red) high

693 intensity. Scale bar: 25 μ m.

694

695 **Fig. 5. *PUCHI*-dependent early repression of meristem establishment.** (A) Hypothetical model

696 showing the role of *PUCHI* at early stages of LRP formation, *PUCHI* acts as a key regulator of

697 spatiotemporal distribution of auxin balance and represses specific meristematic module genes.

698

699 **Fig. S1: LRP phenotype of Col-0 and *puchi-1* LRP during the time-course transcriptomic**

700 **analysis after gravistimulation (hpg).** (A) and (B) Brightfield images showing the LRP stages

701 observed for each timepoint. Time points corresponds to phenotype of the LRP observed in the

702 RNAseq samples. The percentages of occurrence for each LRP stages per time point are shown.

703 (C) Distribution of LRP developmental stages after 18, 24, 30 hours post-gravistimulation (hpg) in

704 Col-0 and *puchi-1* roots. Data are one biological replicate for Col-0 and two biological replicates for

705 *puchi-1*. The number of observed seedlings is indicated (n=X).

706

707 **Fig. S2. GO-terms enrichment during the time-course transcriptomic analysis of LR**

708 **formation in *puchi-1* compared to Col-0 upon gravistimulation.** (A) Distribution of Gene

709 Ontologies among DEGs in *puchi* was analysed using a PANTHER overrepresentation assay and
710 Fisher test followed by a Bonferroni Correction ($p^* < 0.05$). The Heat map shows the GO terms fold
711 enrichment of DEGs for each time point.

712

713 **Figure S3. Time-course transcriptomic analysis in Col-0 and *puchi-1* after gravistimulation.**

714 Heat map of selected gene patterns up- and down-regulated in *puchi-1* compared to Col-0
715 background during the formation of LRP. Statistical analysis on three independent RNAseq
716 replicates were performed using the DESeq2 package and Wald Test: p-value: $* < 0.05$; $** < 0.02$;
717 $*** < 0.01$. Colour code for the heatmap is red for upregulated genes and blue for downregulated
718 genes. Colour code for gene names and AGI numbers indicates the module classification (Orange:
719 module1, Morphogenetic phase and Purple: module 2, Meristematic phase) as described in
720 Lavenus *et al.*, 2015.

721

722 **Fig. S4. Time-course transcriptomic analysis in Col-0 and *puchi-1* upon gravistimulation. (A)**

723 RT-qPCR analysis of *PLT1*, *PLT2*, *PLT3*, *PLT4*, *PLT5* and *PLT7* gene expression levels 24h after
724 lateral root induction NPA/NAA treatment (Himanen *et al.*, 2002) in *puchi-1* and Col-0. Data are
725 represented as mean \pm SEM (standard error of the means), $n=3$ independent biological replicates.
726 Significance was determined using a Student's t test ($* p < 0.05$, $** p < 0.01$, $*** p < 0.001$).
727 Expression pattern of (B-G) *promPLT2:PLT2-YFP* and (H-M) *promPLT3:PLT3-YFP* (green) in
728 *puchi-1* and Col-0 LR primordia. Percentages and numbers indicate the occurrence of the
729 represented pattern over the total number of observations. (B-M) Cell membranes were stained
730 using propidium iodide (magenta). Scale bar: 25 μ m.

731

732 **Figure S5. Identified PUCHI target genes in different datasets. (A)** Venn diagram showing the

733 number of targeted genes by PUCHI using DAPseq (Ronan *et al.*, 2016;
734 http://neomorph.salk.edu/dap_web/pages/index.php), RNAseq analysis in *puchi-1* background
735 after gravistimulation (This paper) and PUCHI-GR inducible system (Trinh *et al.*, 2019). Genes in
736 pPUCHI::PUCHI:GR in *puchi-1* seedlings showed an upregulation (fold change ≥ 1.5 , p-value

737 ≤ 0.05 as determined by Welch two sample t-test) in the following conditions were used: NAA CHX
738 DEX vs NAA CHX. (GR: GLUCOCORTICOID RECEPTOR; DEX: dexamethasone; CHX:
739 cycloheximide). (B) The common gene (red) between the three datasets and 25 genes (Auxin-;
740 cytokinin-; VLCFA-; LR-; meristematic- related and transcription factors) that were common
741 between two datasets (among a full list of 150 genes, Supp. Table 1) were selected and their AGI
742 number, aliases and TAIR summary are described in the table.

743

744 **Figure S6. Expression patterns of the 8 predicted PUCHI target genes.** (A-H) Gene expression
745 patterns in *puchi-1* and Col-0 background during the formation of LRP. Data are means +/- SE of
746 three replicates per time point from the transcriptomic dataset. Statistical analysis on RNAseq
747 replicates were performed using DESeq2 package and Wald Test: p-value: * <0.05 ; ** <0.02 ;
748 *** <0.01 .

749

750 **Fig. S7: Selected gene expression analysis in Col-0 and *puchi-1* after gravistimulation. (A-H)**
751 Gene expression patterns in *puchi-1* and Col-0 background during the formation of LRP. Data are
752 means +/- SE of three replicates per time point from the transcriptomic dataset. Statistical analysis
753 on RNAseq replicates were performed using DESeq2 package and Wald Test: p-value: * <0.05 ;
754 ** <0.02 ; *** <0.01 .

755

756

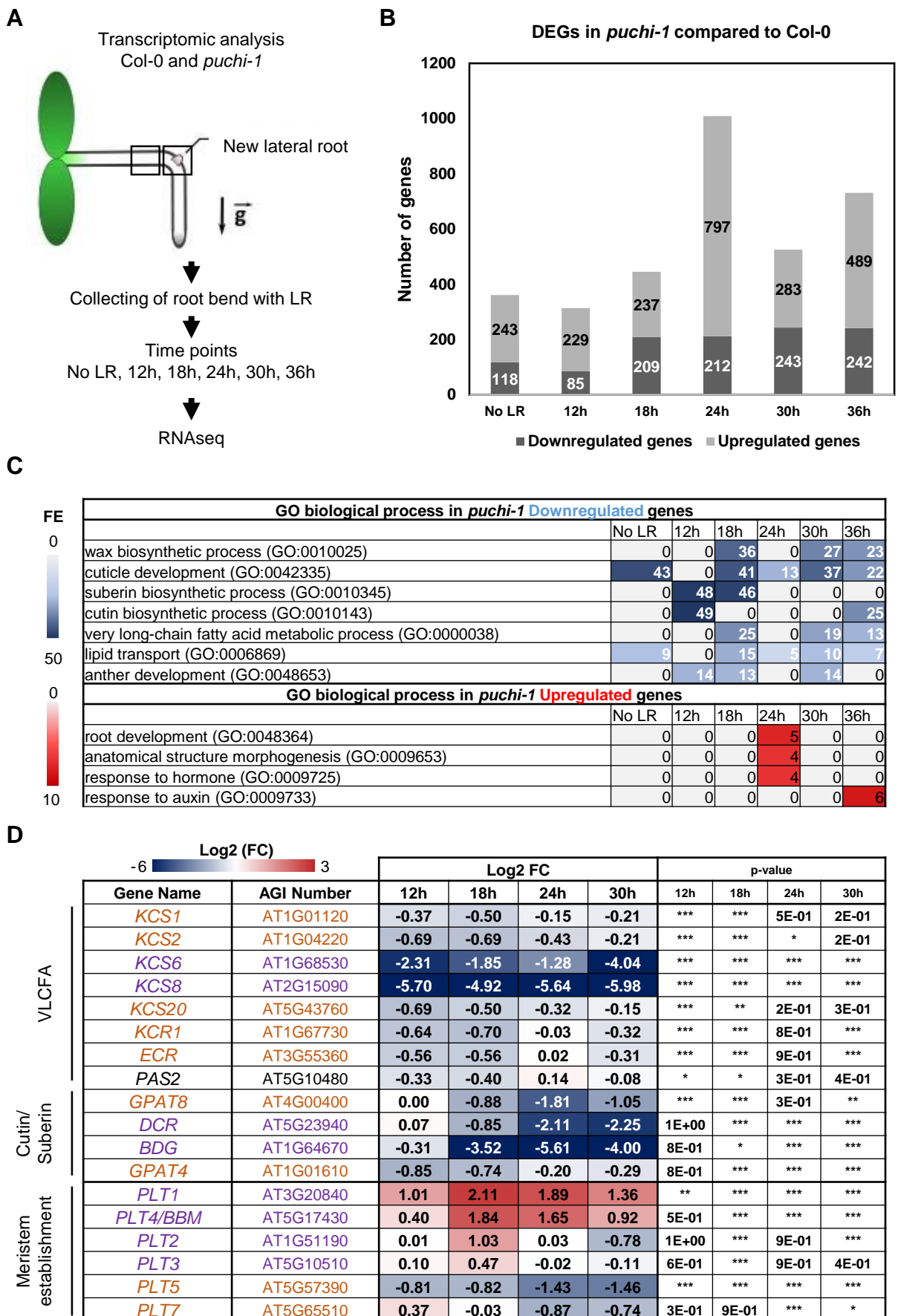


Figure 1. Time-course transcriptomic analysis of LRP formation in Col-0 and *puchi-1* after root gravistimulation. (A) Schematic diagram of the experimental procedure for the RNAseq analysis. (B) Number of differentially expressed genes (DEGs) in *puchi-1* compared to Col-0 at No LR, 12h, 18h, 24h, 30h and 36h after gravistimulation. Genes with a fold-change of up to Log2: +/-1; $p^* < 0.05$ selected. (C) Distribution of elementary Gene Ontologies (GO) among either, upregulated genes or downregulated genes in *puchi* was analysed using a PANTHER overrepresentation assay and Fisher test followed by a Bonferroni Correction ($p^* < 0.05$). The Heat map shows the GO terms fold enrichment (FE) of DEGs for each time point. (D) Heat map of selected gene patterns up- and down-regulated in *puchi-1* compared to Col-0 background during the formation of LRP. Log 2-fold change (FC) of expression in *puchi-1* compared to WT is given. Statistical analysis on three independent RNAseq replicates were performed using the DESeq2 package and Wald Test: p-value: $p^* < 0.05$; $p^{**} < 0.02$; $p^{***} < 0.01$. Colour code for the heatmaps in (C) and (D) are red for upregulated genes and blue for downregulated genes. Colour code for gene names in (D) indicates the module classification (Orange: module1, Morphogenetic phase and Purple: module 2, Meristematic phase) as described in Lavenus *et al.*, 2015.

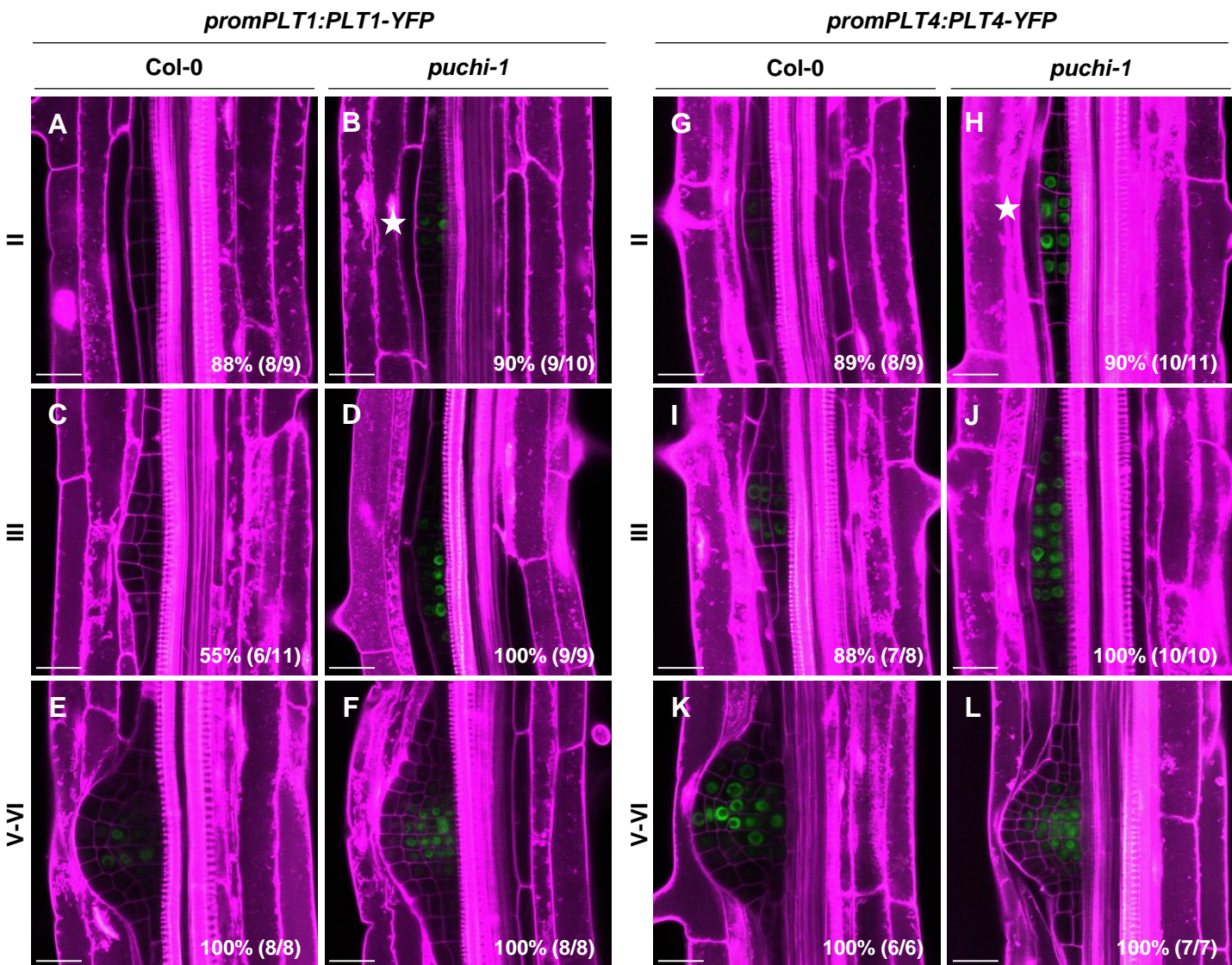


Figure 2. *PUCHI* loss of function results in distinct expression patterns of meristematic phase regulator *PLT* genes during LRP development. (A-F) and (G-L) Expression pattern of *promPLT1:PLT1-YFP* and *promPLT4:PLT4-YFP* (green) respectively in *puchi-1* and Col-0 LR primordia. Stars indicate earlier detected signal expression during LRP outgrowth. Percentages and numbers indicate the occurrence of the represented pattern over the total number of observations. Cell walls were stained using propidium iodide (magenta). Scale bar: 25 μ m.

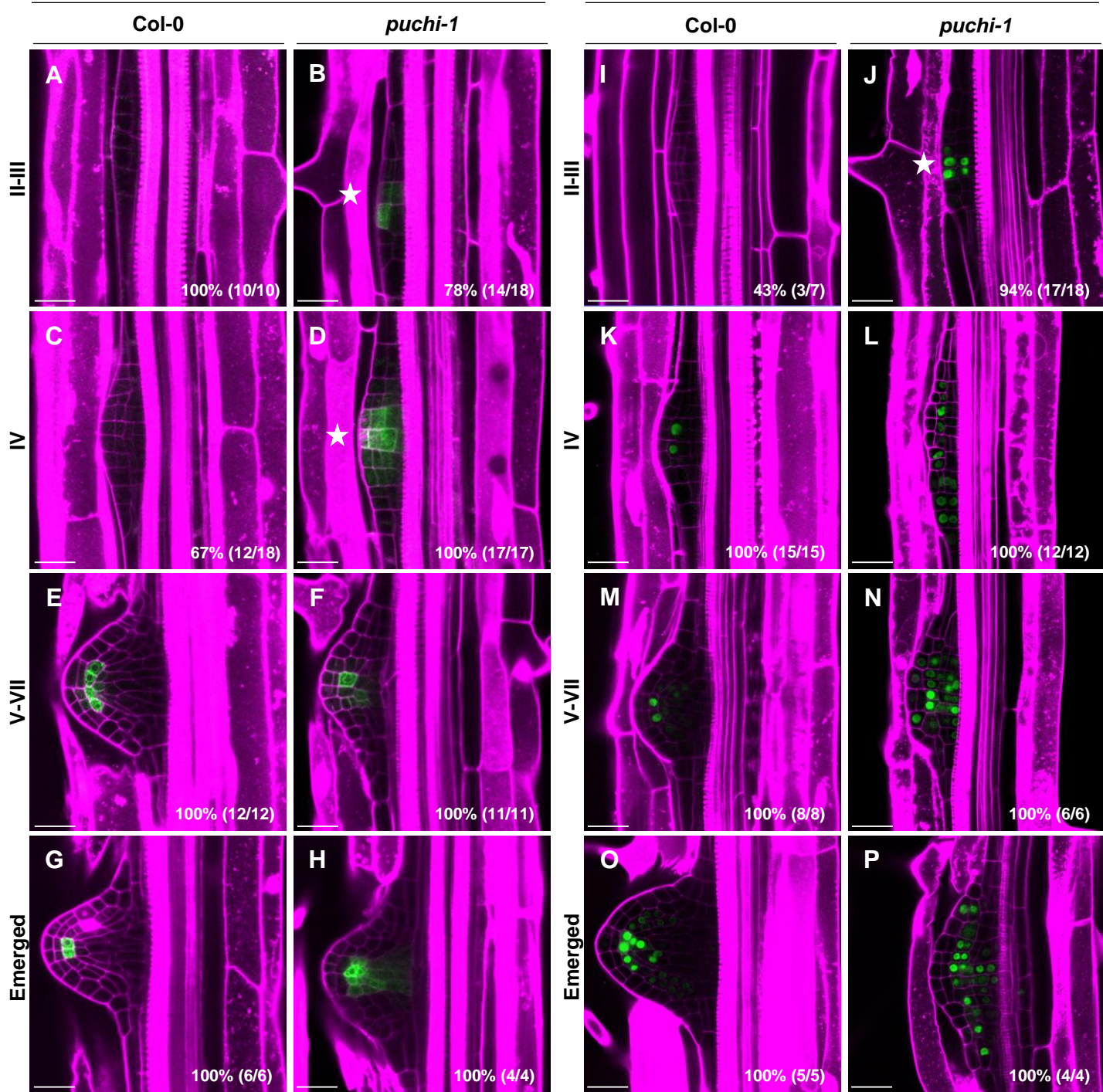
*QC25::CFP**promWOX5::nls:GFP*

Figure 3. *PUCHI* loss of function impacts QC marker gene expression patterns during LRP formation. Confocal microscopy images of expression of QC reporters (A-H) *QC25::CFP* and (I-P) *promWOX5::nls:GFP* (green) in LRP in Col-0 and *puchi-1*. Stars indicate earlier detected signal expression during LRP outgrowth. Percentages and numbers indicate the occurrence of the represented pattern over the total number of observations. Cell walls were stained using propidium iodide (magenta). Scale bar: 25 μ m.

A

| | | Log2 (FC) | | | | p-value | | | |
|--------------|------------|-----------|------|------|------|---------|---------|-----|-----|
| | | 0 | 1 | | 3 | | | | |
| Gene Name | AGI Number | 12h | 18h | 24h | 30h | 12h | 18h | 24h | 30h |
| <i>PIN1</i> | AT1G73590 | 0.24 | 0.49 | 0.88 | 0.65 | * | *** | *** | *** |
| <i>PIN4</i> | AT2G01420 | 0.28 | 0.17 | 0.90 | 0.74 | 2.9E-01 | 3.9E-01 | *** | *** |
| <i>PIN7</i> | AT1G23080 | 0.22 | 0.50 | 0.45 | 0.54 | 2.3E-01 | *** | *** | *** |
| <i>PIN3</i> | AT1G70940 | 0.47 | 0.59 | 0.75 | 0.67 | *** | *** | *** | *** |
| <i>LAX3</i> | AT1G77690 | 0.44 | 0.42 | 0.71 | 0.63 | ** | *** | *** | *** |
| <i>IAA2</i> | AT3G23030 | 0.21 | 0.41 | 0.34 | 0.76 | 1.7E-01 | *** | * | *** |
| <i>IAA29</i> | AT4G32280 | 1.14 | 0.87 | 0.60 | 1.01 | *** | *** | * | *** |

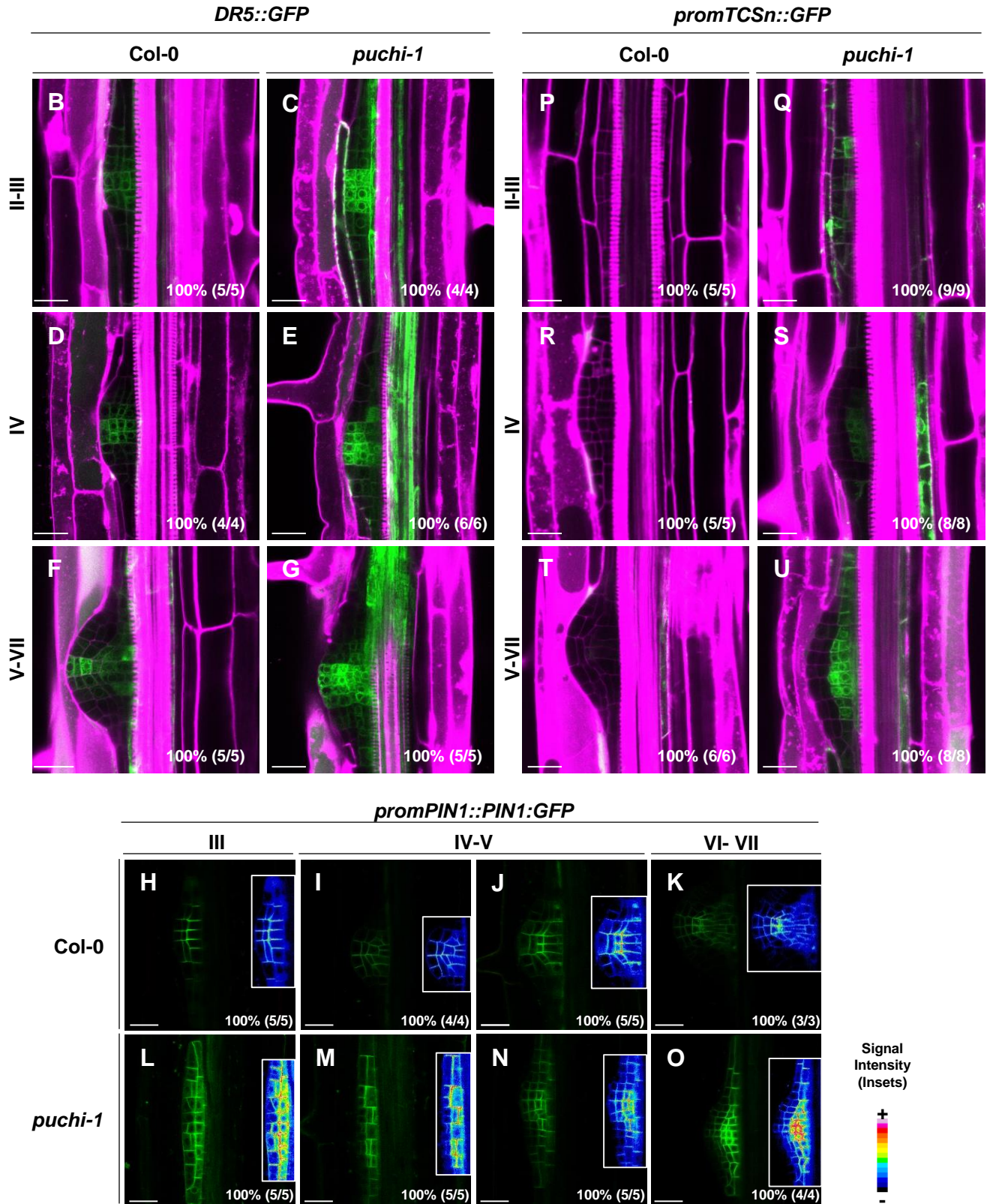


Figure 4. *PUCHI* loss of function alters auxin and cytokinin signal distribution in developing LRP. (A) Heat map of selected auxin transporter gene patterns upregulated in *puchi-1* compared to Col-0 background during LRP formation. Log 2-fold change (FC) of expression in *puchi-1* compared to WT is given. Statistical analysis on the three independent RNAseq replicates were performed using the DESeq2 package and Wald Test: p -value: $p^* < 0.05$; $p^{**} < 0.02$; $p^{***} < 0.01$. (B-G) *DR5::GFP* (green), (H-O) *promPIN1::PIN1:GFP* (green) and (P-U) *promTCSn::GFP* (green) expression during LR development. Percentages and numbers indicate the occurrence of the represented pattern over the total number of observations. (B-U) Cell walls were stained using propidium iodide (magenta). (H-O) (Inset) Signal intensity monitor. (blue) low intensity; (red) high intensity. Scale bar: 25 μ m.

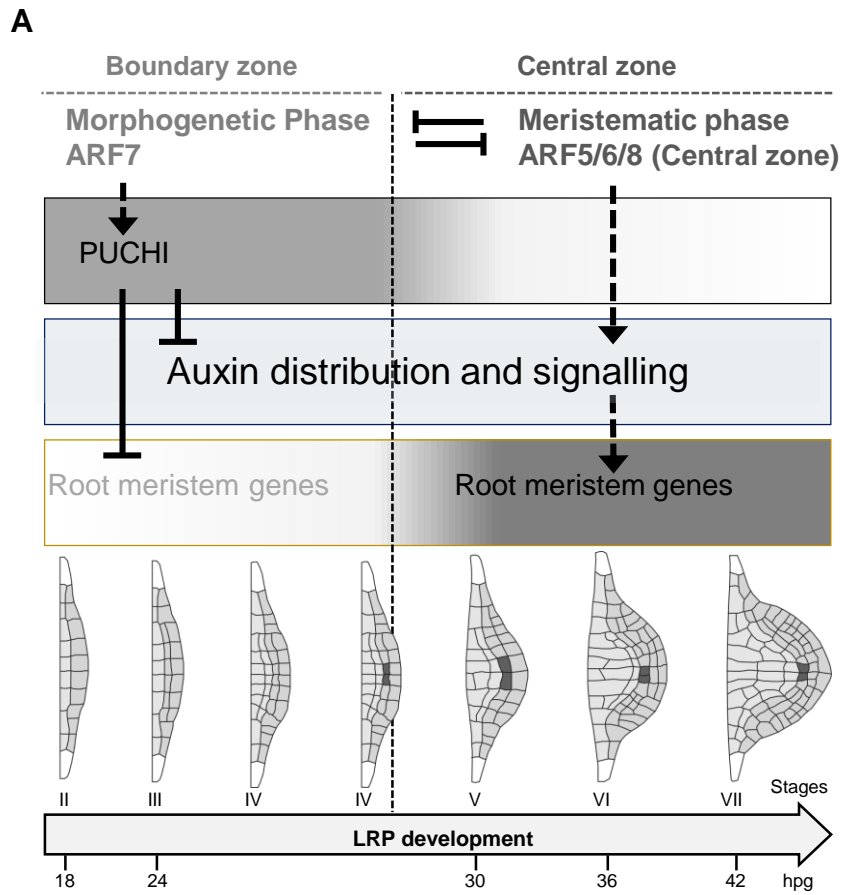
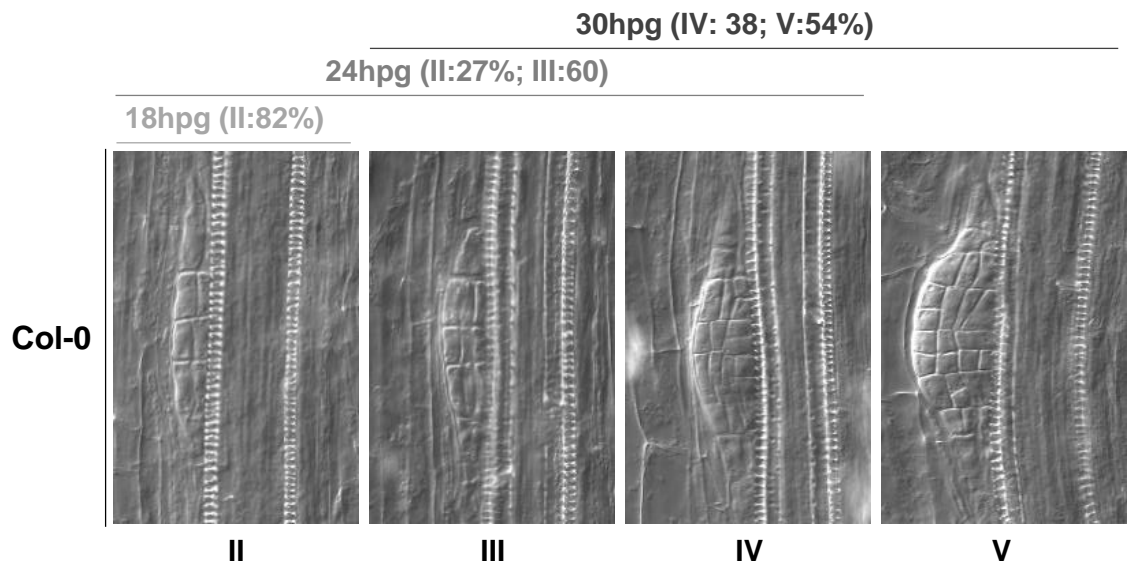
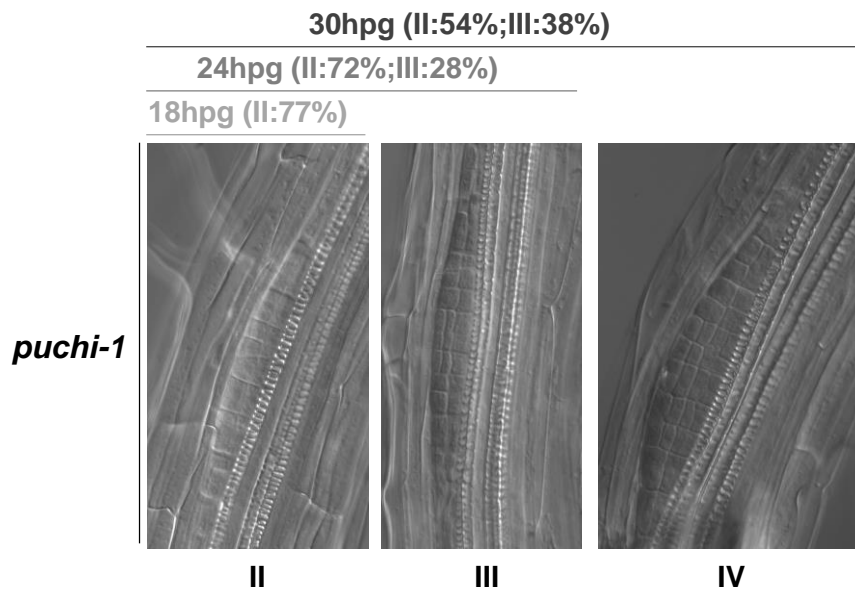


Fig. 5. *PUCHI*-dependent early repression of meristem establishment. (A) Hypothetical model showing the role of *PUCHI* at early stages of LRP formation, *PUCHI* acts as a key regulator of spatiotemporal distribution of auxin balance and represses specific meristematic module genes.

A



B



C

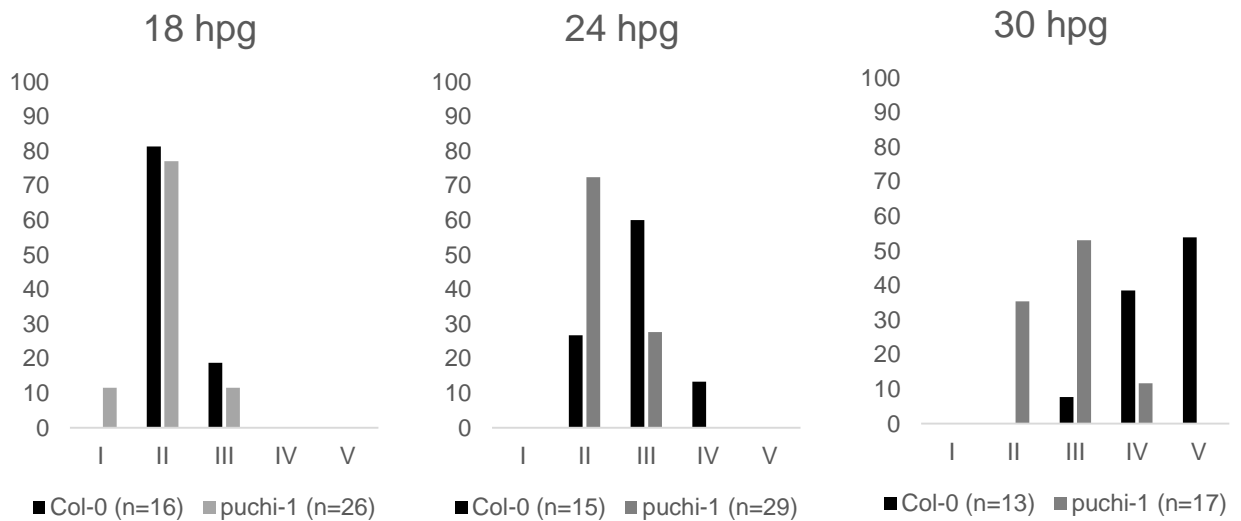


Fig. S1: LRP phenotype of Col-0 and *puchi-1* LRP during the time-course transcriptomic analysis after gravistimulation (hpg). (A) and (B) Brightfield images showing the LRP stages observed for each timepoint. Time points corresponds to phenotype of the LRP observed in the RNAseq samples. The percentages of occurrence for each LRP stages per time point are shown. (C) Distribution of LRP developmental stages after 18, 24, 30 hours post-gravistimulation (hpg) in Col-0 and *puchi-1* roots. Data are one biological replicate for Col-0 and two biological replicates for *puchi-1*. The number of observed seedlings is indicated (n=X).

A

| GO biological process enrichment in <i>puchi-1</i> Downregulated genes | | | | | | |
|--|-------|-----|-----|-----|-----|-----|
| | No LR | 12h | 18h | 24h | 30h | 36h |
| wax biosynthetic process (GO:0010025) | 0 | 0 | 36 | 0 | 27 | 23 |
| cuticle development (GO:0042335) | 43 | 0 | 41 | 13 | 37 | 22 |
| suberin biosynthetic process (GO:0010345) | 0 | 48 | 46 | 0 | 0 | 0 |
| cutin biosynthetic process (GO:0010143) | 0 | 49 | 0 | 0 | 0 | 25 |
| fatty acid biosynthetic process (GO:0006633) | 0 | 0 | 0 | 0 | 10 | 0 |
| fatty acid metabolic process (GO:0006631) | 0 | 9 | 0 | 0 | 0 | 0 |
| very long-chain fatty acid metabolic process (GO:0000038) | 0 | 0 | 25 | 0 | 19 | 13 |
| lipid transport (GO:0006869) | 9 | 0 | 15 | 5 | 10 | 7 |
| response to fatty acid (GO:0070542) | 0 | 0 | 0 | 5 | 0 | 0 |
| lipid biosynthetic process (GO:0008610) | 5 | 0 | 0 | 0 | 0 | 0 |
| triterpenoid metabolic process (GO:0006722) | 0 | 0 | 0 | 0 | 0 | 22 |
| phyllome development (GO:0048827) | 5 | 0 | 0 | 0 | 0 | 3 |
| anther development (GO:0048653) | 0 | 14 | 13 | 0 | 14 | 0 |
| secondary metabolic process (GO:0019748) | 0 | 0 | 0 | 5 | 0 | 0 |
| response to stress (GO:0006950) | 2 | 0 | 0 | 0 | 0 | 0 |
| cellular response to hypoxia (GO:0071456) | 0 | 0 | 0 | 8 | 0 | 0 |
| response to salicylic acid (GO:0009751) | 0 | 0 | 0 | 5 | 0 | 0 |
| cell differentiation (GO:0030154) | 0 | 0 | 0 | 0 | 0 | 3 |
| GO biological process enrichment in <i>puchi-1</i> Upregulated genes | | | | | | |
| | No LR | 12h | 18h | 24h | 30h | 36h |
| root development (GO:0048364) | 0 | 0 | 0 | 5 | 0 | 0 |
| anatomical structure morphogenesis (GO:0009653) | 0 | 0 | 0 | 4 | 0 | 0 |
| cell growth (GO:0016049) | 0 | 0 | 0 | 6 | 0 | 0 |
| response to hormone (GO:0009725) | 0 | 0 | 0 | 4 | 0 | 0 |
| response to auxin (GO:0009733) | 0 | 0 | 0 | 0 | 0 | 6 |
| regulation of hormone levels (GO:0010817) | 0 | 0 | 0 | 0 | 0 | 6 |
| response to organic substance (GO:0010033) | 4 | 0 | 0 | 0 | 0 | 0 |
| response to wounding (GO:0009611) | 0 | 0 | 0 | 0 | 7 | 0 |
| cellular response to endogenous stimulus (GO:0071495) | 0 | 0 | 0 | 5 | 0 | 0 |
| response to jasmonic acid (GO:0009753) | 0 | 0 | 0 | 0 | 9 | 0 |
| response to fatty acid (GO:0070542) | 0 | 0 | 0 | 0 | 9 | 0 |
| regulation of transcription, DNA-templated (GO:0006355) | 0 | 0 | 0 | 0 | 0 | 3 |

Fig. S2. GO-terms enrichment during the time-course transcriptomic analysis of LR formation in *puchi-1* compared to *Col-0* upon gravistimulation. (A) Distribution of Gene Ontologies among DEGs in *puchi* was analysed using a PANTHER overrepresentation assay and Fisher test followed by a Bonferroni Correction ($p^* < 0.05$). The Heat map shows the GO terms fold enrichment of DEGs for each time point.

| Gene Name | AGI Number | Log2 FC | | | | | | p-value | | | | | |
|------------------------------|------------|---------|-------|-------|-------|-------|-------|---------|---------|---------|---------|---------|---------|
| | | No LR | 12h | 18h | 24h | 30h | 36h | No LR | 12h | 18h | 24h | 30h | 36h |
| QC specific | | | | | | | | | | | | | |
| NAP | AT1G69490 | 2,33 | -0,06 | 1,08 | 0,14 | 2,98 | 2,02 | *** | 9,4E-01 | 9,4E-02 | 7,9E-01 | *** | *** |
| WIP4 | AT3G20880 | 0,78 | 0,83 | 5,13 | 4,41 | 1,24 | 0,68 | 3,9E-01 | 5,6E-01 | *** | *** | * | 8,1E-02 |
| DUF9 | AT5G23780 | 0,48 | 0,36 | 1,10 | 0,48 | 0,61 | 0,14 | 3,7E-01 | 4,2E-01 | *** | 1,1E-01 | 1,3E-01 | 6,4E-01 |
| NPY4 | AT2G23050 | 0,48 | 0,39 | 0,88 | 1,96 | 1,19 | 0,72 | 5,6E-01 | 6,1E-01 | *** | *** | *** | *** |
| APL4 | AT2G21590 | -0,29 | 0,34 | 1,12 | 1,18 | 1,06 | 0,11 | 7,6E-01 | 5,4E-01 | * | *** | ** | 8,0E-01 |
| WOX5 | AT3G11260 | 0,10 | 0,55 | 0,64 | -0,50 | -0,75 | -0,98 | 7,8E-01 | 1,1E-01 | *** | * | *** | *** |
| Morphogenesis | | | | | | | | | | | | | |
| FEZ | AT1G26870 | 0,18 | 0,39 | -0,18 | 2,13 | 1,22 | -0,70 | 8,6E-01 | 6,3E-01 | 8,0E-01 | * | ** | * |
| SHR | AT4G37650 | 0,14 | 0,06 | 0,31 | 0,46 | 0,33 | 0,36 | 5,3E-01 | 6,0E-01 | *** | *** | *** | *** |
| SCR | AT3G54220 | -0,07 | 0,06 | -0,07 | 0,27 | -0,06 | -0,04 | 8,2E-01 | 6,5E-01 | 5,3E-01 | 6,4E-02 | 5,7E-01 | 7,3E-01 |
| WER/MYB66 | AT5G14750 | -1,06 | 0,55 | -0,17 | 0,65 | -1,38 | -2,44 | 4,3E-01 | 2,7E-01 | 6,2E-01 | 3,1E-01 | *** | *** |
| MIR166b | AT3G61897 | 0,08 | 0,04 | 0,55 | -0,18 | -1,11 | 1,39 | 9,6E-01 | 9,7E-01 | 4,5E-01 | 8,4E-01 | 3,1E-01 | 7,4E-02 |
| KAN4/ATS | AT5G42630 | -1,27 | 0,10 | -0,63 | -0,98 | -2,02 | -1,64 | ** | 7,6E-01 | * | *** | *** | *** |
| Auxin transport | | | | | | | | | | | | | |
| LAX3 | AT1G77690 | 0,41 | 0,44 | 0,42 | 0,71 | 0,63 | 0,48 | 2,7E-01 | ** | *** | *** | *** | *** |
| Auxin signalling | | | | | | | | | | | | | |
| ARF2 | AT5G62000 | 0,36 | 0,06 | 0,18 | 0,09 | 0,22 | 0,37 | *** | 5,9E-01 | 1,6E-01 | 4,7E-01 | ** | *** |
| MP/ARF5 | AT1G19850 | -0,13 | -0,10 | 0,08 | 0,11 | 0,44 | 0,24 | 7,0E-01 | 6,7E-01 | 5,6E-01 | 3,2E-01 | *** | 1,1E-01 |
| ARF7 | AT5G20730 | -0,11 | -0,07 | -0,06 | -0,02 | -0,02 | 0,00 | 5,5E-01 | 5,6E-01 | 5,2E-01 | 7,6E-01 | 8,2E-01 | 9,9E-01 |
| ARF9 | AT4G23980 | 0,24 | 0,10 | 0,24 | 0,05 | 0,15 | 0,22 | 2,1E-01 | 3,2E-01 | 6,6E-02 | 6,3E-01 | 1,6E-01 | 6,8E-02 |
| ARF11 | AT2G46530 | 0,14 | 0,09 | 0,31 | -0,07 | 0,20 | 0,18 | 6,2E-01 | 7,1E-01 | 2,1E-01 | 7,2E-01 | 3,4E-01 | 3,9E-01 |
| ARF19 | AT1G19220 | 0,13 | 0,14 | 0,17 | 0,35 | 0,17 | 0,27 | 4,8E-01 | 2,4E-01 | 8,9E-02 | *** | 9,5E-02 | * |
| ETT | AT2G33860 | -0,03 | 0,08 | 0,05 | -0,28 | -0,28 | -0,06 | 8,6E-01 | 5,7E-01 | 7,2E-01 | 4,3E-02 | *** | 4,7E-01 |
| ARF4 | AT5G60450 | -0,11 | 0,52 | 0,49 | -0,02 | 0,24 | 0,10 | 3,8E-01 | *** | *** | 8,7E-01 | * | 4,2E-01 |
| ARF6 | AT1G30330 | 0,06 | 0,21 | 0,24 | 0,26 | 0,09 | -0,07 | 8,7E-01 | 1,6E-01 | * | * | 3,8E-01 | 5,4E-01 |
| ARF17 | AT1G77850 | 0,16 | 0,25 | 0,24 | -0,12 | -0,06 | 0,05 | 3,7E-01 | 8,2E-02 | 8,1E-02 | 3,5E-01 | 7,3E-01 | 7,3E-01 |
| IAA11 | AT4G28640 | 0,09 | 0,14 | 0,22 | 0,25 | 0,43 | 0,58 | 7,5E-01 | 2,8E-01 | 1,9E-01 | * | *** | *** |
| IAA13 | AT2G33310 | 0,51 | 0,32 | 0,60 | 0,55 | 0,53 | 0,51 | *** | ** | *** | *** | *** | *** |
| IAA2 | AT3G23030 | 0,86 | 0,21 | 0,41 | 0,34 | 0,76 | 1,06 | *** | 1,7E-01 | *** | * | *** | *** |
| IAA29 | AT4G32280 | 1,21 | 1,14 | 0,87 | 0,60 | 1,01 | 1,71 | 1,0E-01 | *** | *** | * | *** | *** |
| IAA5 | AT1G15580 | -0,32 | 0,84 | 1,04 | 1,33 | 0,53 | 1,06 | 6,3E-01 | 1,1E-01 | 8,7E-02 | 8,6E-02 | 3,4E-01 | * |
| SLR/IAA14 | AT4G14550 | 0,19 | 0,23 | -0,01 | 0,50 | 0,32 | -0,03 | 4,4E-01 | 1,0E-01 | 9,3E-01 | *** | * | 8,9E-01 |
| IAA19 | AT3G15540 | 0,36 | 0,30 | 0,54 | -0,17 | 0,25 | 0,12 | 5,1E-01 | 1,5E-01 | *** | 1,2E-01 | 2,4E-01 | 5,4E-01 |
| SHY2 | AT1G04240 | 0,80 | 0,15 | 0,32 | 0,41 | 0,59 | 0,71 | *** | 3,8E-01 | 6,2E-02 | *** | *** | *** |
| Auxin homeostasis | | | | | | | | | | | | | |
| GH3.1 | AT2G14960 | 1,19 | 0,94 | 1,51 | 0,49 | 0,42 | 0,12 | *** | *** | *** | *** | * | 5,0E-01 |
| YDK1/GH3.2 | AT4G37390 | 1,53 | 0,47 | 0,77 | 0,55 | 0,59 | 1,17 | *** | * | *** | 1,1E-01 | *** | *** |
| GH3.3 | AT2G23170 | 2,32 | 0,61 | 0,88 | 1,09 | 1,60 | 2,08 | *** | 4,0E-01 | *** | *** | *** | *** |
| GH3.5 | AT4G27260 | 1,24 | 0,85 | 1,17 | 0,87 | 0,80 | 1,09 | *** | *** | *** | *** | *** | *** |
| DAO1 | AT1G14130 | 0,13 | -0,57 | -0,87 | -0,39 | -0,36 | -0,19 | 3,9E-01 | *** | *** | ** | *** | 1,3E-01 |
| VLCA and Cuticle | | | | | | | | | | | | | |
| CDEF1 | AT4G30140 | 1,07 | -0,71 | 0,43 | 0,20 | 0,49 | 1,19 | 4,6E-01 | * | 5,2E-01 | 8,2E-01 | ** | *** |
| MPK14 | AT4G36450 | 0,29 | 0,46 | 0,62 | 0,71 | 1,15 | 0,56 | 4,8E-01 | 1,8E-01 | 1,2E-01 | * | * | 2,1E-01 |
| ERF13 | AT2G44840 | 0,51 | -0,57 | -0,31 | -1,81 | 0,92 | 0,12 | 3,3E-01 | 6,0E-01 | 8,3E-01 | 1,6E-01 | 1,6E-01 | 9,4E-01 |
| Signalling | | | | | | | | | | | | | |
| GLV6 | AT2G03830 | -0,16 | 0,77 | 1,11 | 1,11 | 0,11 | -0,72 | 8,5E-01 | ** | *** | *** | 7,6E-01 | *** |
| MAKR4 | AT2G39370 | 0,88 | 0,64 | 0,90 | 1,20 | 1,00 | 1,99 | 1,5E-01 | *** | *** | *** | *** | *** |
| MKK4 | AT1G51660 | -0,03 | -0,27 | -0,08 | -0,52 | -0,04 | 0,06 | 9,4E-01 | 2,3E-01 | 8,0E-01 | * | 8,0E-01 | 8,2E-01 |
| MKK5 | AT3G21220 | -0,37 | -0,19 | -0,21 | -0,34 | -0,01 | -0,31 | 7,6E-02 | 2,7E-01 | 1,4E-01 | *** | 9,7E-01 | *** |
| MPK3 | AT3G45640 | 0,32 | -0,56 | -0,25 | -0,99 | 0,51 | 0,06 | 5,4E-01 | 3,7E-01 | 7,3E-01 | *** | 8,9E-02 | 9,2E-01 |
| TOLS2 | AT4G37295 | 0,32 | 0,56 | 0,67 | 0,34 | 0,22 | 0,55 | 1,9E-01 | ** | *** | * | 1,5E-01 | *** |
| Transcription factors | | | | | | | | | | | | | |
| FLP/MYB124 | AT1G14350 | -0,65 | -0,77 | -0,68 | -0,71 | -0,39 | -0,54 | 1,5E-01 | *** | *** | *** | 4,3E-02 | *** |
| GATA23 | AT5G26930 | 1,08 | 1,55 | 1,79 | 2,80 | 2,38 | 3,57 | 4,5E-01 | *** | *** | *** | *** | *** |
| LBD16 | AT2G42430 | -0,09 | -0,93 | -0,89 | -1,11 | -0,86 | -0,44 | 8,3E-01 | *** | *** | *** | *** | *** |
| LBD18 | AT2G45420 | 0,09 | 0,27 | 0,59 | 0,20 | 0,42 | 0,20 | 8,5E-01 | 1,5E-01 | *** | 3,5E-01 | * | 4,8E-01 |
| LBD29 | AT3G58190 | 0,94 | 0,39 | 0,62 | 0,82 | 0,99 | 1,13 | *** | 1,7E-01 | *** | *** | *** | *** |
| Cytokinins | | | | | | | | | | | | | |
| CRF1 | AT4G11140 | -1,68 | -2,64 | -2,88 | -2,40 | -2,50 | -2,24 | *** | *** | *** | *** | *** | *** |
| CRF3 | AT5G53290 | 0,09 | 0,58 | 0,71 | 0,54 | 0,65 | 0,38 | 7,0E-01 | *** | *** | *** | *** | *** |
| CRF2 | AT4G23750 | 0,56 | 0,48 | 0,67 | 0,40 | 0,16 | -0,18 | 1,9E-01 | 5,7E-02 | *** | ** | 2,5E-01 | 2,8E-01 |
| CRF4 | AT4G27950 | -0,51 | 0,29 | 0,22 | 0,66 | 0,38 | -0,21 | 2,4E-01 | 4,9E-01 | 4,2E-01 | * | 7,7E-02 | 5,4E-01 |
| APT5 | AT5G11160 | -1,05 | 0,10 | 0,23 | -0,14 | -0,14 | -0,52 | 1,4E-01 | 9,1E-01 | 6,3E-01 | 6,3E-01 | 6,1E-01 | 6,9E-02 |
| AHP6 | AT1G80100 | -1,59 | -1,24 | -1,02 | -0,87 | -0,37 | -1,56 | * | 5,6E-02 | * | 7,9E-02 | 4,5E-01 | *** |
| ARR5 | AT3G48100 | -0,73 | -0,53 | -0,12 | 0,10 | 0,02 | -0,85 | ** | 8,3E-02 | 3,7E-01 | 5,2E-01 | 9,5E-01 | *** |
| ARR14 | AT2G01760 | -0,04 | -0,51 | 0,18 | 0,09 | 0,38 | 0,03 | 9,6E-01 | 3,0E-01 | 7,5E-01 | 8,0E-01 | 2,5E-01 | 8,9E-01 |
| ARR18 | AT5G58080 | 1,38 | N/A | N/A | -0,46 | -0,04 | N/A | 2,7E-01 | N/A | N/A | 7,1E-01 | 9,8E-01 | N/A |
| ARR15 | AT1G74890 | -2,12 | 0,42 | 0,58 | 1,15 | -0,99 | -0,45 | | 4,3E-01 | 2,1E-01 | 1,6E-02 | 1,9E-01 | 7,0E-01 |
| ARR7 | AT1G19050 | -0,15 | -0,07 | -0,07 | -0,13 | -0,15 | -0,67 | 8,6E-01 | 7,5E-01 | 7,2E-01 | 4,4E-01 | 4,4E-01 | *** |
| IPT7 | AT3G23630 | -0,60 | -0,45 | -0,50 | -0,64 | -0,56 | -0,61 | 1,7E-01 | * | *** | *** | *** | ** |
| IPT1 | AT1G68460 | -2,00 | 0,62 | -1,47 | 0,40 | -1,01 | -2,40 | 2,4E-01 | 6,8E-01 | 2,3E-01 | 7,4E-01 | 4,4E-01 | * |
| IPT3 | AT3G63110 | -0,62 | 0,06 | -0,06 | -0,34 | -0,42 | -0,27 | 6,7E-02 | 7,3E-01 | 7,0E-01 | 1,0E-01 | ** | 2,7E-01 |
| CKX1 | AT2G41510 | 0,24 | -0,24 | 0,01 | 0,89 | 0,82 | 1,31 | 6,8E-01 | 4,3E-01 | 9,6E-01 | *** | *** | *** |
| CKX6 | AT3G63440 | 0,72 | 0,94 | 1,23 | 1,21 | 1,21 | 1,18 | *** | *** | *** | *** | *** | *** |
| CKX5 | AT1G75450 | -0,71 | 0,12 | 0,16 | -0,26 | -0,09 | -0,47 | ** | 6,7E-01 | 2,5E-01 | 1,7E-01 | 7,1E-01 | ** |
| CKX2 | AT2G19500 | -0,37 | N/A | N/A | N/A | -1,75 | -1,77 | 8,7E-01 | N/A | N/A | N/A | 4,0E-01 | 1,2E-01 |
| LOG3 | AT2G37210 | 1,32 | 0,29 | 1,80 | 1,42 | 1,74 | 0,86 | * | 4,9E-01 | *** | *** | *** | *** |

Module 1 (Lavenus *et al.*, 2015)

Module 2 (Lavenus *et al.*, 2015)

Figure S3. Time-course transcriptomic analysis in Col-0 and *puchi-1* after gravistimulation. Heat map of selected gene patterns up- and down-regulated in *puchi-1* compared to Col-0 background during the formation of LRP. Statistical analysis on three independent RNAseq replicates were performed using the DESeq2 package and Wald Test: p-value: * <0.05 ; ** <0.02 ; *** <0.01 . Colour code for the heatmap is red for upregulated genes and blue for downregulated genes. Colour code for gene names and AGI numbers indicates the module classification (Orange: module1, Morphogenetic phase and Purple: module 2, Meristematic phase) as described in Lavenus *et al.*, 2015.

A

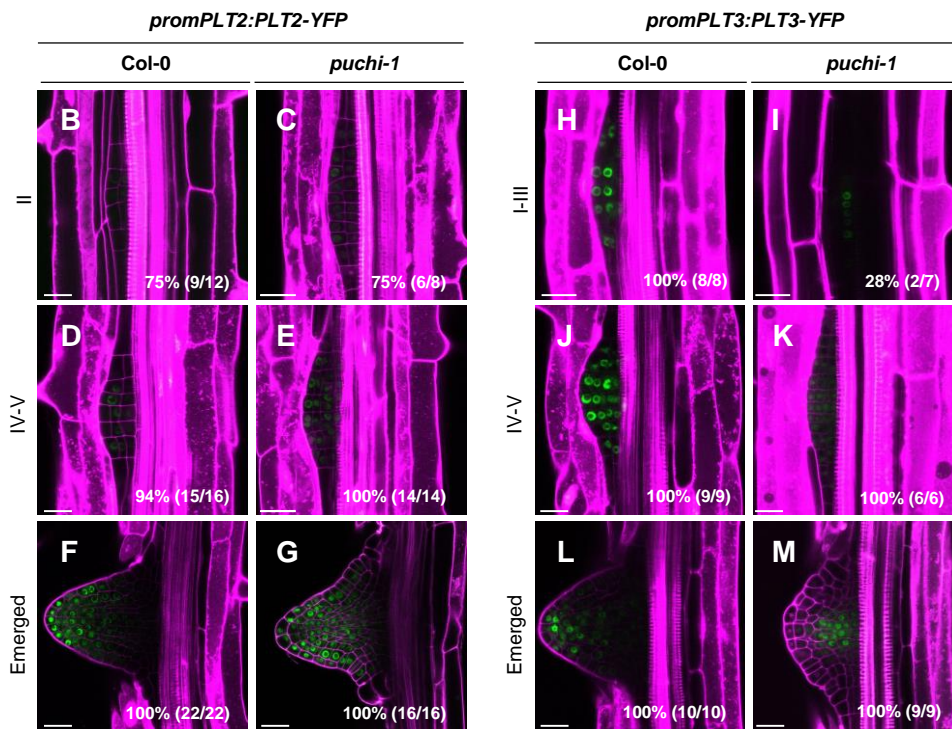
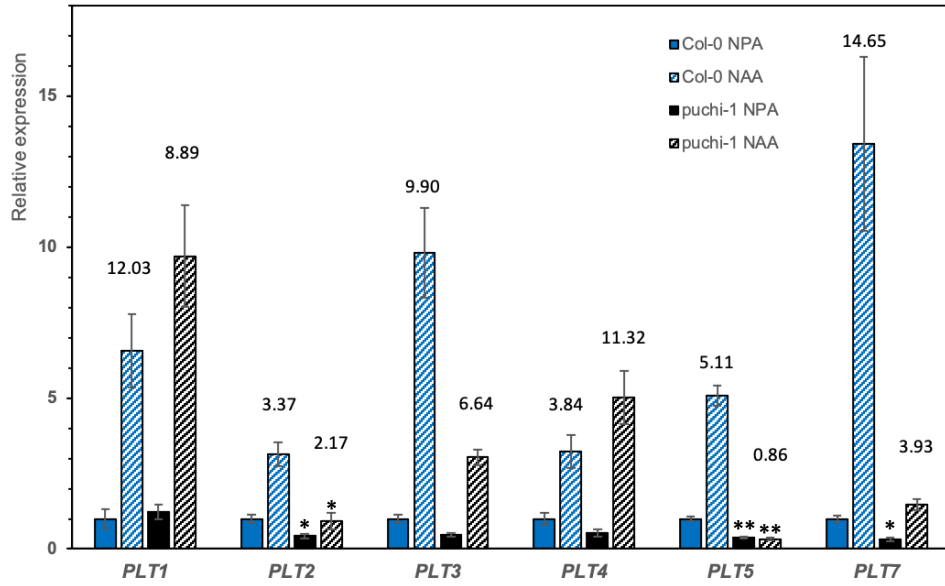
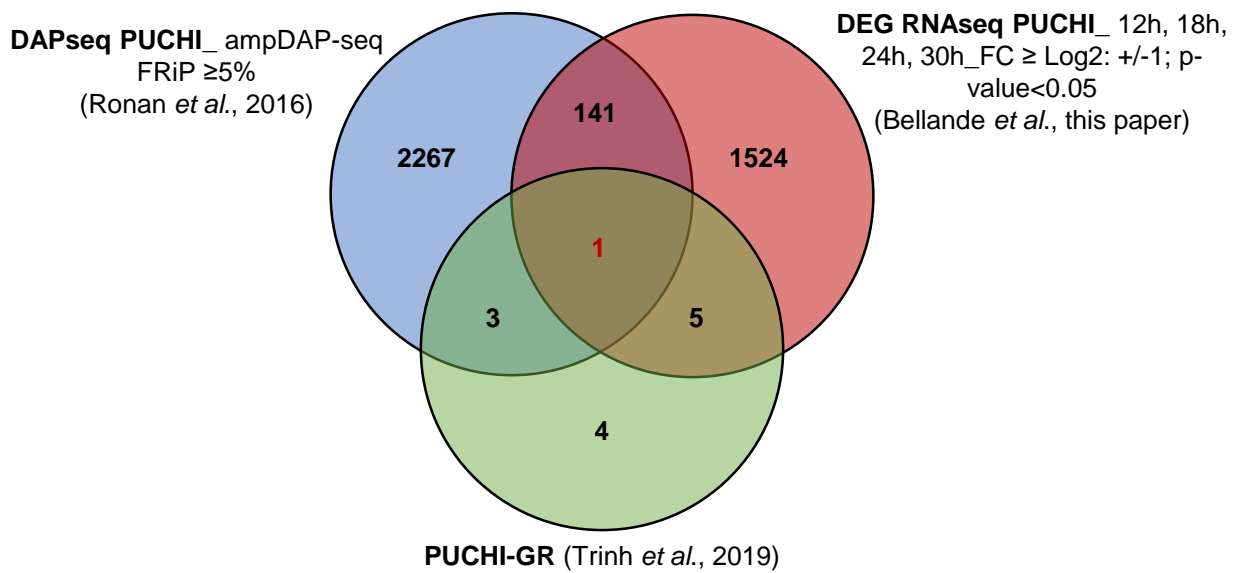


Fig. S4. Time-course transcriptomic analysis in Col-0 and *puchi-1* upon gravistimulation. (A) RT-qPCR analysis of *PLT1*, *PLT2*, *PLT3*, *PLT4*, *PLT5* and *PLT7* gene expression levels 24h after lateral root induction NPA/NAA treatment (Himanen *et al.*, 2002) in *puchi-1* and Col-0. Data are represented as mean \pm SEM (standard error of the means), n=3 independent biological replicates. Significance was determined using a Student's t test (* $p < 0.05$, ** $p < 0.01$, *** $p < 0.001$). Expression pattern of (B-G) *promPLT2:PLT2-YFP* and (H-M) *promPLT3:PLT3-YFP* (green) in *puchi-1* and Col-0 LR primordia. Percentages and numbers indicate the occurrence of the represented pattern over the total number of observations. (B-M) Cell membranes were stained using propidium iodide (magenta). Scale bar: 25 μ m.

A



B

| AGI number | TAIR Aliases | TAIR Summary |
|------------|----------------|--|
| AT4G11140 | CRF1 | Encodes a member of the ERF (ethylene response factor) subfamily B-5 of ERF/AP2 transcription factor family. The protein contains one AP2 domain. There are 7 members in this subfamily. CRF proteins relocate to the nucleus in response to cytokinin. |
| AT3G51060 | SRS1, STY1 | A member of SHI gene family. Arabidopsis thaliana has ten members that encode proteins with a RING finger-like zinc finger motif. Despite being highly divergent in sequence, many of the SHI-related genes are partially redundant in function and synergistically promote gynoecium, stamen and leaf development in Arabidopsis. STY1/STY2 double mutants showed defective style, stigma as well as serrated leaves. Binds to the promoter of YUC4 and YUC8 (binding site ACTCTAC) |
| AT1G19790 | SRS7 | A member of SHI gene family. Arabidopsis thaliana has ten members that encode proteins with a RING finger-like zinc finger motif. Despite being highly divergent in sequence, many of the SHI-related genes are partially redundant in function and synergistically promote gynoecium, stamen and leaf development in Arabidopsis. |
| AT2G28500 | LBD11 | |
| AT3G56400 | WRKY70 | Member of WRKY Transcription Factor |
| AT4G29230 | NAC075 | NAC domain protein involved in negative regulation of flowering. |
| AT5G53950 | ANAC098, CUC2 | Transcriptional activator of the NAC gene family, with CUC1 redundantly required for embryonic apical meristem formation, cotyledon separation and expression of STM. Proper timing of CUC2 expression is required to maintain the phyllotactic pattern initiated in the meristem. CUC2 expression in leaf sinus region is required for serration and the extent of serration is modulated by mir164A mediated repression of CUC2. Together with CUC3-DA1-UBP15 part of a regulatory module which controls the initiation of axillary meristems, thereby determining plant architecture. Regulates the axillary meristem initiation, directly binding to the DA1 promoter. |
| AT1G28360 | ERF12 | encodes a member of the ERF (ethylene response factor) subfamily B-1 of ERF/AP2 transcription factor family (ERF12). The protein contains one AP2 domain. There are 15 members in this subfamily including ATERF-3, ATERF-4, ATERF-7, and leafy petiole. Regulates floral development. |
| AT1G12610 | DDF1 | Encodes a member of the DREB subfamily A-1 of ERF/AP2 transcription factor family (DDF1). The protein contains one AP2 domain. There are six members in this subfamily, including CBF1, CBF2, and CBF3. Overexpression of this gene results in delayed flowering and dwarfism, reduction of gibberellic acid biosynthesis, and increased tolerance to high levels of salt. This gene is expressed in all tissues examined, but most abundantly expressed in upper stems. Overexpression of this gene is also correlated with increased expression of GA biosynthetic genes and RD29A (a cold and drought responsive gene). Under salt stress it induces the expression of GAOX7, which encodes a C20-GA inhibitor. |
| AT2G20880 | ERF53 | Encodes ERF53, a drought-induced transcription factor. Belongs to the AP2/ERF superfamily, and has a highly conserved AP2 domain. Regulates drought-responsive gene expressions by binding to the GCC box and/or dehydration-responsive element (DRE) in the promoter of downstream genes. Overexpression of AtERF53 driven by the CaMV35S promoter resulted in an unstable drought-tolerant phenotype in T2 transgenic plants. Involved in heat shock response. |
| AT5G24110 | WRKY30 | member of WRKY Transcription Factor |
| AT5G47220 | ERF2 | Encodes a member of the ERF (ethylene response factor) subfamily B-3 of ERF/AP2 transcription factor family (ATERF-2). The protein contains one AP2 domain. Functions as activator of GCC box-dependent transcription. Positive regulator of JA-responsive defense genes and resistance to <i>F. oxysporum</i> and enhances JA inhibition of root elongation. |
| AT1G29670 | GDSL1 | GDSL-motif esterase/acyltransferase/lipase. Enzyme group with broad substrate specificity that may catalyze acyltransfer or hydrolase reactions with lipid and non-lipid substrates. The mRNA is cell-to-cell mobile. |
| AT2G38110 | GPAT6 | bifunctional sn-glycerol-3-phosphate 2-O-acyltransferase/phosphatase. Involved in cutin assembly. |
| AT3G16370 | | GDSL-motif esterase/acyltransferase/lipase. Enzyme group with broad substrate specificity that may catalyze acyltransfer or hydrolase reactions with lipid and non-lipid substrates. The mRNA is cell-to-cell mobile. |
| AT5G56970 | CKX3 | It encodes a protein whose sequence is similar to cytokinin oxidase/dehydrogenase, which catalyzes the degradation of cytokinins. |
| AT4G26200 | ACCS7, ACS7, | Member of a family of proteins in Arabidopsis that encode 1-Amino-cyclopropane-1-carboxylate synthase, an enzyme involved in ethylene biosynthesis. Not expressed in response to IAA. |
| AT1G51500 | ABCG12, CER5 | Encodes an ABC transporter involved in cuticular wax biosynthesis. Lines carrying recessive mutations in this locus have weakly glaucous stem surface, and relative elevated secondary alcohols and ketones. |
| AT1G43160 | ERF113, RAP2.6 | encodes a member of the ERF (ethylene response factor) subfamily B-4 of ERF/AP2 transcription factor family (RAP2.6). The protein contains one AP2 domain. There are 7 members in this subfamily. |
| AT5G57390 | AIL5, PLT5 | Encodes a member of the AP2 family of transcriptional regulators. May be involved in germination and seedling growth. Mutants are resistant to ABA analogs and are resistant to high nitrogen concentrations.essential for the developmental transition between the embryonic and vegetative phases in plants. Overexpression results in the formation of somatic embryos on cotyledons. It is also required to maintain high levels of PIN1 expression at the periphery of the meristem and modulate local auxin production in the central region of the SAM which underlies phyllotactic transitions. Acts redundantly with PLT3 and 7 in lateral root pattern formation. |
| AT2G14960 | GH3.1 | encodes a protein similar to IAA-amido synthases. Lines carrying an insertion in this gene are hypersensitive to auxin. |
| AT1G24470 | KCR2 | Encodes one of the two Arabidopsis homologues to YBR159w encoding a <i>S. cerevisiae</i> beta-ketoacyl reductase (KCR), which catalyzes the first reduction during VLCFA (very long chain fatty acids, >18 carbon) elongation: KCR1 (At1g67730), KCR2 (At1g24470). Complementation of the yeast ybr159Delta mutant demonstrated that the two KCR proteins are divergent and that only AtKCR1 can restore heterologous elongase activity similar to the native yeast KCR gene. |
| AT1G46264 | HSFB4, SCZ | Encodes SCHIZORIZA, a member of Heat Shock Transcription Factor (Hsf) family. Functions as a nuclear factor regulating asymmetry of stem cell divisions. |
| AT1G71030 | MYBL2 | Encodes a putative myb family transcription factor. In contrast to most other myb-like proteins its myb domain consists of a single repeat. A proline-rich region potentially involved in transactivation is found in the C-terminal part of the protein. Its transcript accumulates mainly in leaves. |
| AT4G36260 | SRS2, STY2 | A member of SHI gene family. Arabidopsis thaliana has ten members that encode proteins with a RING finger-like zinc finger motif. Despite being highly divergent in sequence, many of the SHI-related genes are partially redundant in function and synergistically promote gynoecium, stamen and leaf development in Arabidopsis. Encodes protein with a single zinc finger motif and a members of a small gene family of putative transcription factors in which the SHORT INTERNODES (SHI) gene is found. STY2/STY1 double mutants showed defective style, stigma as well as serrated leaves. |

Figure S5. Identified PUCHI target genes in different datasets. (A) Venn diagram showing the number of targeted genes by PUCHI using DAPseq (Ronan *et al.*, 2016; http://neomorph.salk.edu/dap_web/pages/index.php), RNAseq analysis in *puchi-1* background after gravistimulation (this paper) and PUCHI-GR inducible system (Trinh *et al.*, 2019). Genes in pPUCHI::PUCHI:GR in *puchi-1* seedlings showed an upregulation (fold change ≥ 1.5 , p-value ≤ 0.05 as determined by Welch two sample t-test) in the following conditions: NAA CHX DEX vs NAA CHX. (GR: GLUCOCORTICOID RECEPTOR; DEX: dexamethasone; CHX: cycloheximide). (B) The common gene (red) between the three datasets and 25 genes (Auxin-, cytokinin-, VLCFA-, LR-, meristematic- related and transcription factors) that were common between two datasets (among the 150 genes, see suppl. Table 1 for details) were selected and their AGI number, aliases and TAIR summary are shown in the table.

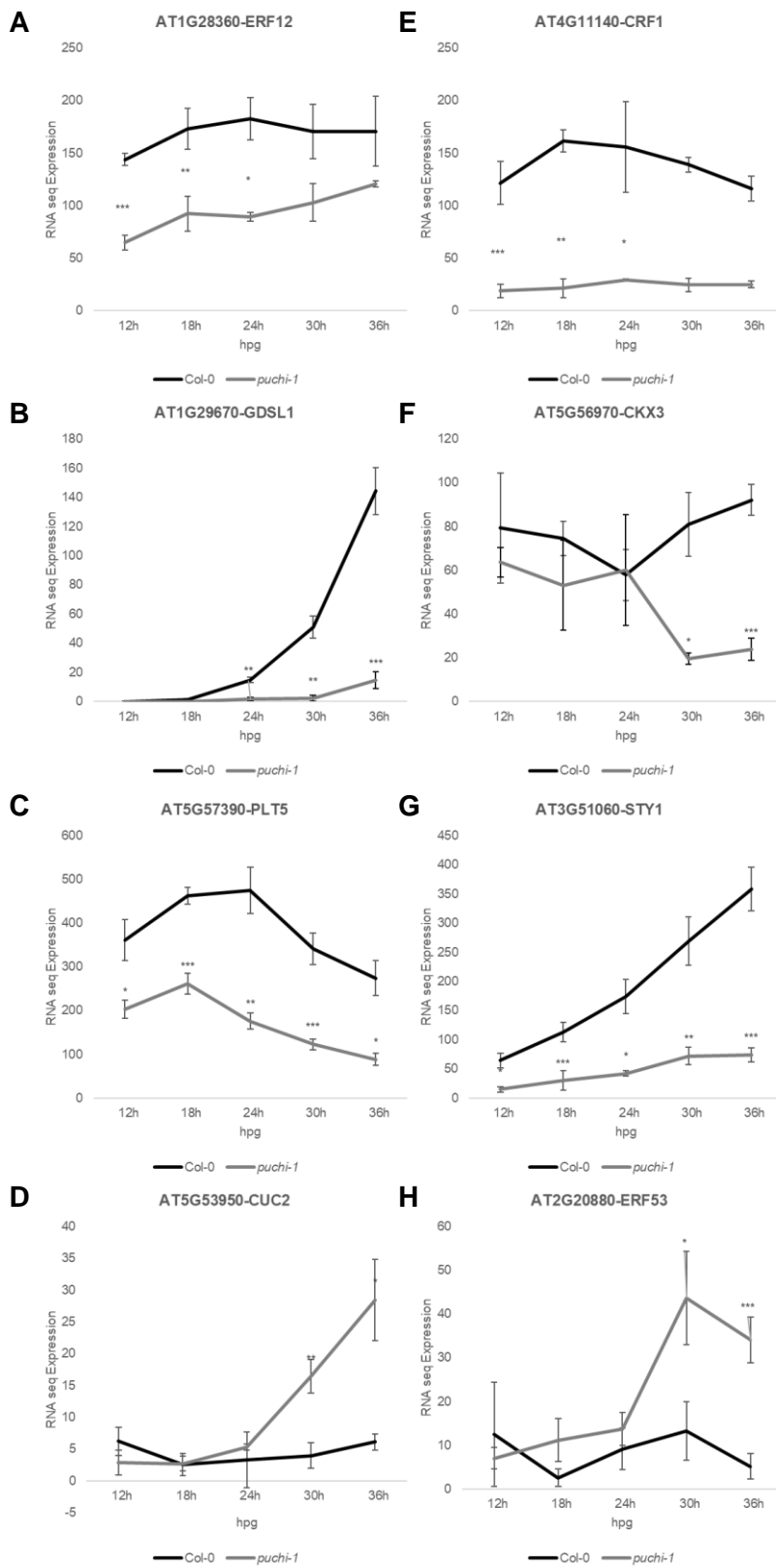


Figure S6. Expression patterns of the 8 predicted PUCHI target genes. (A-H) Gene expression patterns in *puchi-1* and Col-0 background during the formation of LRP. Data are means \pm SE of three replicates per time point from the transcriptomic dataset. Statistical analysis on RNAseq replicates were performed using DESeq2 package and Wald Test: p-value: * <0.05 ; ** <0.02 ; *** <0.01 .

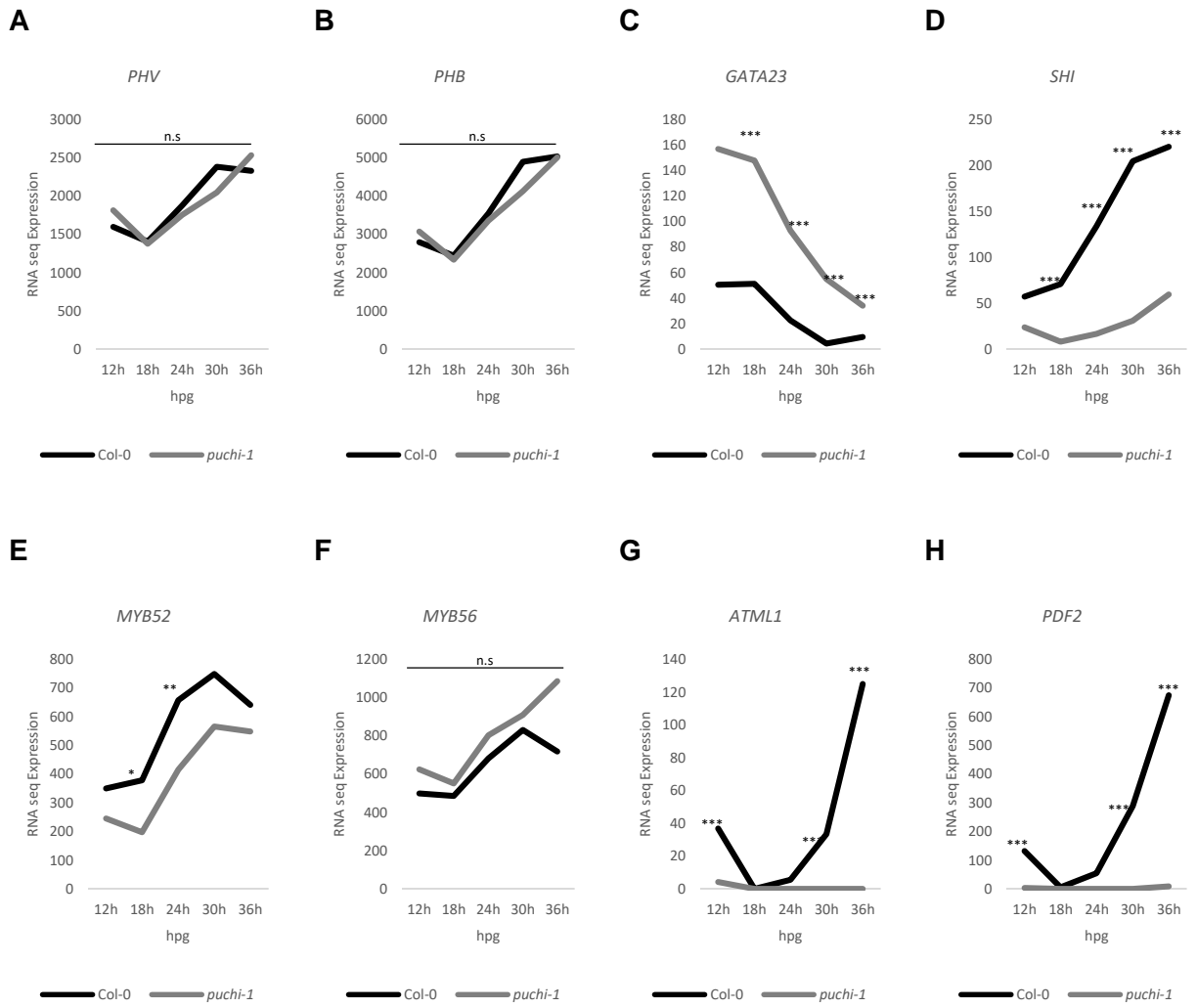


Fig. S7: Selected gene expression analysis in Col-0 and *puchi-1* after gravistimulation. (A-H) Gene expression patterns in *puchi-1* and Col-0 background during the formation of LRP. Data are means \pm SE of three replicates per time point from the transcriptomic dataset. Statistical analysis on RNAseq replicates were performed using DESeq2 package and Wald Test: p-value: * <0.05 ; ** <0.02 ; *** <0.01 .